Principle Component Analysis Decomposition of Core Collapse Supernovae Gravitational Waveforms

Christopher V. Griffith[1], Patrick Sutton[2]

[1]Department of Astronomy, University of California, Berkeley

[2]Department of Physics, Cardiff University

August 10, 2009

Abstract

This paper discusses the use of Principle Component Analysis(PCA) as a method to decompose theoretical supernovae waveform catalogs and describe them with minimal eigenvectors. We discuss the core-collapse catalogs developed by Harald Dimmelmeier and Christian Ott and decompose each using the PCA method. We also produce eigenvectors which describe all five catalogs of theoretical waveforms. We find that all of the catalogs can be described very accurately using ten eigenvectors. We also find the coefficients of the eigenvectors can accurately determine the type of the waveform.

1   Introduction

Current gravitational wave detectors are becoming much more sensitive and a detection is becoming an ever present reality. With the new technology present at the detectors, one must think of the best way to discover the source of the signal. Many theorists including Christian Ott and Harald Dimmelmeier have produced theoretical supernovae gravitational waveforms which describe very different physical phenomena. The catalogs of these waveforms are large and contain hundreds of waveforms. Each waveform contains different input parameters including initial mass, density, and angular momentum. The computation costs of testing every waveform on the detected signal would prove to be high and time consuming.

We propose the use of Principle Component Analysis (PCA) developed by Ik Siong Heng (Heng 2009) as a way to decompose the catalogs into a small number of orthonormal eigenvectors therefore reducing the computation costs. We decompose various catalogs include Dimmelmeier's 2002 catalog (Dimmelmeier et al. 2002) , 2007 catalog (Dimmelmeier et al. 2007), 2008 catalog (Dimmelmeier et al. 2008) Zwerger and Mueller 1996 catalog (Zwerger & Mueller 1997) and Ott and Burrow's 2003 catalog (Ott et al. 2004). We then combined all of the waveforms into one catalog and decomposed them. We also discuss the reconstruction of the waveforms from the eigenvectors and how the coefficients of the eigenvectors can determine parameters of the waveform. In this paper, I will discuss the procedure of PCA decomposition and the sampling that was used. I will then discuss the types and waveforms used in our analysis and finally discuss the results and applications of the procedure.

2 Core Collapse Supernovae

Core-collapse supernovae originate from very massive stars of at least 8 solar masses. The stars undergo core collapse at the very end of their nuclear burning stage and create an explosion of their envelope. If the progenitor star is greater than 25 solar masses then a black hole is likely to form after the explosion. If it is between 8 to 25 solar masses than a neutron star will form.

2.1 Types of Core-collapse Supernovae

There are three types of supernovae whose mechanism is core collapse.

- Type II - The supernovae's spectra contains strong hydrogen Balmer lines. Appear near star forming galaxies and have not been seen in elliptical galaxies. Their individual spectra show a lot of variation and sub types have been introduced. Light curve is mostly powered by shock ionization.

- Type Ib - The spectra shows no hydrogen Balmer lines, weak or absent Si II lines and strong He I lines. They are core collapse supernovae with progenitor stars more massive than 20 solar masses that have lost their hydrogen envelopes due to stellar wind or a companion star. (Ott 2003)

- Type Ic - The spectra contain weak or absent hydrogen, helium and silicon. They are believed to be core-collapse supernovae that have lost their hydrogen and helium envelopes.

2.2 Collapse Mechanism

Like every star, massive stars get their energy by fusing hydrogen into helium. The difference in mass is then converted into energy. However when a massive star reaches the end of its hydrogen supply, hydrostatic equilibrium is broken and the star contracts and begins fusing helium. Since the star is so massive the contraction can cause the core of the star to reach energies to fuse heavier elements. This contracting process continues until the star fuses iron, which has the highest binding energy of nucleons and cannot be fused. The silicon shell surrounding the iron core continues to fuse iron and add to the core's mass. The star remains stable until the iron core reaches the Chandrasekhar mass and collapses. The star then explodes and releases energy on the order of 10^{51} erg.

3 Gravitational Waveforms

3.1 Phases

The waveforms discussed in this paper have three defined phases: the infall phase, bounce phase and ring down phase. The initial parameters of the simulation such as initial mass of the star or angular momentum determine the behavior of the waveform in each phase.

- Infall Phase - The initial collapse of core from gravitational instability. Outer core falls supersonically and lasts 30ms - 100ms

- Bounce Phase - The Equation of State stiffens and becomes repulsive or when centrifugal forces dominate over gravitational forces. The core overshoots equilibrium and bounces back. Lasts $\sim$1 ms

- Ring Down Phase - If centrifugal forces remain small then the core rapidly settles down to a new equilibrium. Lasts $\sim$10ms. If core collapse is only predominately stopped by centrifugal forces the core experience several distinct sequences of infall, bounce and re-expansion separated by $\sim$50ms and it eventually reaches equilibrium.

3.2   Types

There are three types of waveforms discussed in this paper.

- Type I: Regular Collapse- During the infall, density increases and exceeds nuclear matter density. The core slightly re-expands and rings down to equilibrium (Figure 1).

- Type II: Multiple Bounce Collapse - Centrifugal forces halt collapse at densities below nuclear matter density. Multiple bounces are seen at successive lower amplitudes (Figure 2).

- Type III: Rapid Core Collapse- Similar to Type I except bounce and equilibrium densities are slightly higher and post bounce pulsations of inner core are strongly suppressed. Overall amplitude is smaller than Type I (Figure 3).

A supernovae's gravitational waveform depends strongly on its central angular velocity and mass. A Type II waveform with most likely arise from a star with a high rotation rate and a Type I from a star with little initial rotation. A Type III occurs in a star with a low mass inner core to allow for fast collapse.

4   Method

4.1   Resampling the Waveforms

Each catalog had a different method of sampling the waveforms. In order to make things easier in our calculations and our results more universal between catalogs we resampled all of the waveforms at 4096 Hz. This procedure made the samples equally spaced and identical for every waveform. We also made the length of the waveforms equal by padding the ends of the waveforms with zeros.

4.2   Aligning the Waveforms

The first step in producing the eigenvectors was aligning the waveforms so we could decompose them in the most optimal way. We accomplished this by determining which two waveforms had the biggest inner product and therefore looked most
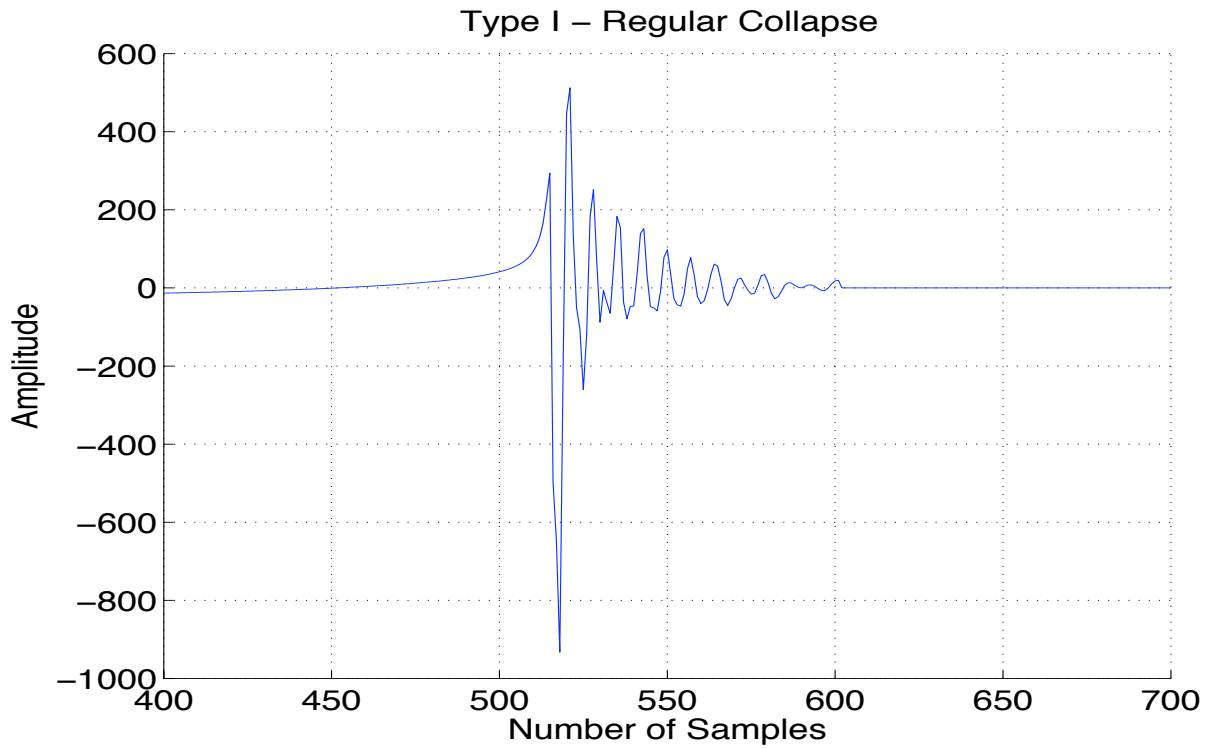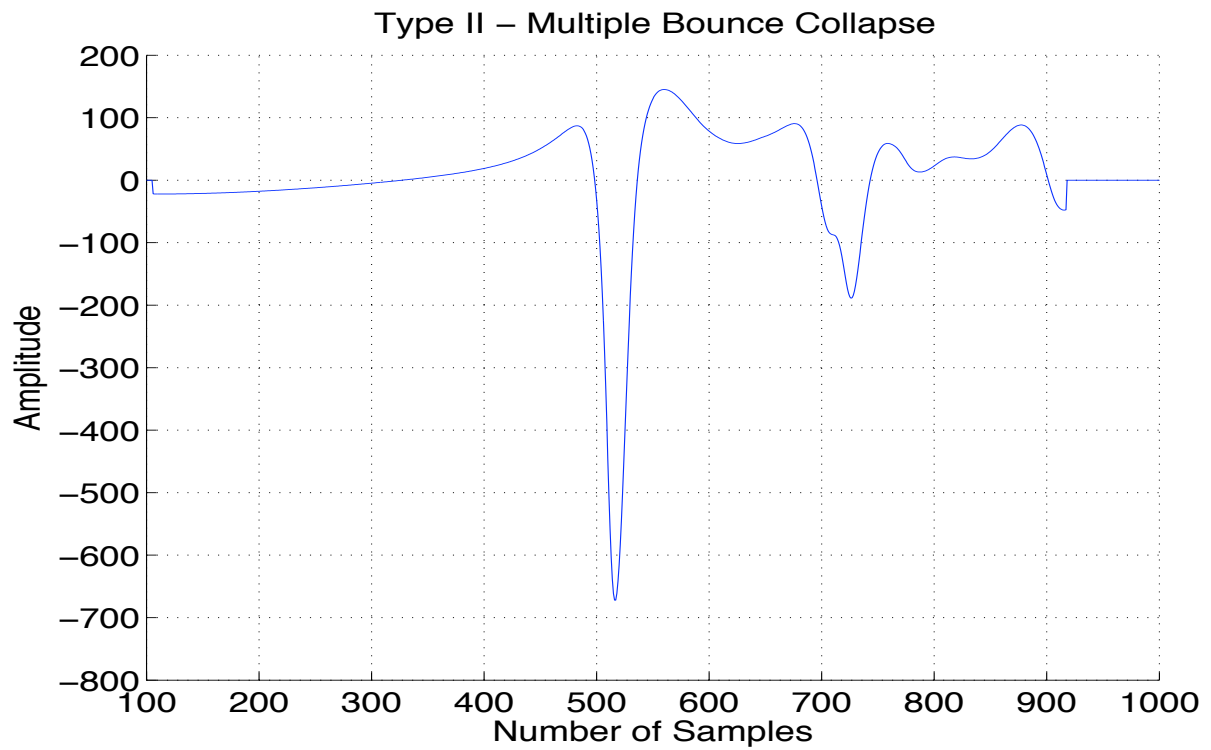
Figure 1: Type I - Regular Core Collapse

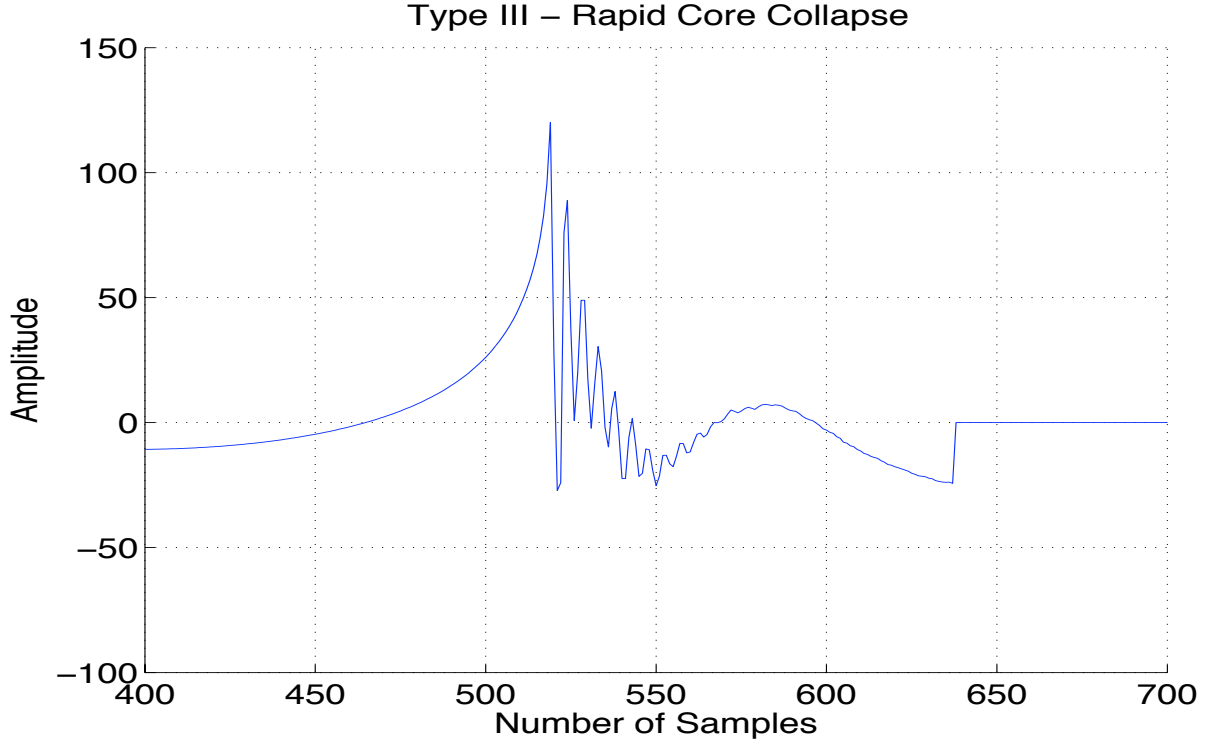Figure 2: Type II - Multiple Bounce Collapse

Figure 3: Type III - Rapid Core Collapse

like each other. When we took the inner product of the two waveforms we included the noise weighting of the LIGO detector. When we incorporate the noise weighting the equation for the inner product becomes

$$Y(t) = 2 \int_{-\infty}^{\infty} \frac{X1(f)X2(f)^* e^{i2\pi ft}}{S(|f|)} df \tag{1}$$

Where $S(|f|)$ is a vector of noise values expected from LIGO at different frequencies and X1 and X2 are the waveforms. The numerator of the above equation arises from the definition of a Fourier transform:

$$\int_0^T X(t)X(t+\tau)dt = X(t)X(t)e^{i2\pi t} \tag{2}$$

Where τ is the time shift of the waveform. The inclusion of the noise weighting ensured we were concentrating our inner product on frequencies where LIGO has the best sensitivity. We then shifted the waveforms accordingly and lined up the waveforms with the waveform that best matched it. We found that this method gave us the biggest eigenvalues and therefore the strongest eigenvectors.

4.3 Principle Component Analysis

This method was first applied to gravitational waves by Ik Siong Heng(Heng 2009). In Principle Component Analysis, a basis set is formed by finding the eigenvectors of the covariance matrix of the data set rather than the entire data set. Let us arrange the waveforms in a matrix **H** such that each column is a waveform. For M waveforms with length N the matrix

has dimensions $N \times M$. The equation for the covariance matrix of H is therefore:

$$\mathbf{C} = \frac{1}{M}\mathbf{H}\mathbf{H}^T \tag{3}$$

Where C is the covariance matrix with dimensions $N \times N$ for waveforms with length N. The normalized eigenvectors of $\mathbf{C}$ form a set of basis vectors that span the parameter space defined by the waveforms in $\mathbf{H}$. The eigenvalue of each eigenvector in the covariance matrix tells us how each vector spans the parameter space of the catalog. Therefore the eigenvectors are ranked by their corresponding eigenvalue.

However since supernovae waveforms contain 1000 or more samples finding the eigenvectors of the covariance matrix mentioned above would be very computationally expensive. A way to avoid this is implement a linear algebra trick. If we first calculate the eigenvectors, $\mathbf{v}$, of $\mathbf{H}^T\mathbf{H}$ such that

$$\mathbf{H}^T\mathbf{H}\mathbf{v}_i = \lambda_i\mathbf{v}_i \tag{4}$$

where λ_i is the corresponding eigenvalue to each eigenvector. Then if we multiply each side by $\mathbf{H}$ we have

$$\mathbf{H}\mathbf{H}^T\mathbf{H}\mathbf{v}_i = \lambda_i\mathbf{H}\mathbf{v}_i \tag{5}$$

If we rewrite Equation 3 so that $\mathbf{C} = \mathbf{H}\mathbf{H}^T$ then $\mathbf{H}\mathbf{v}_i$ are the eigenvectors of the covariance matrix. So for $M \ll N$ we can find the eigenvectors of the covariance matrix by first calculating the eigenvectors of the much smaller $\mathbf{H}^T\mathbf{H}$ which is $M \times M$. This method significantly reduces the computing costs. We also incorporated the noise weighting of LIGO and therefore found the eigenvectors of $\mathbf{H}^T\frac{1}{S}\mathbf{H}$ where S is a vector of noise values at different frequencies according to LIGO's sensitivity. After calculating the eigenvectors we threw out any vectors with corresponding values that were less than .0001 times the first eigenvalue. We concluded these vectors to be insignificant in our calculations.

5 Analysis

5.1 Dimmelmeier 2002 Newtonian Waveforms

The first catalog we decomposed was Dimmelmeier's 2002 catalog. Dimmelmeier's 2002 catalog has two categories of waveforms those that use Newtonian gravity and those that use relativistic. In both categories, the Einstein equations used to generate the waveforms were formulated using the conformally flat metric approximation and the corresponding hydrodynamic equations are written as a first order flux-conservative hyperbolic system. Collapse was generated by decreasing the adiabatic index to a fixed value. Any microphysics like electron capture and neutrino transport were neglected (Dimmelmeier et al. 2002). We first ran our scripts on his Newtonian waveforms. The Newtonian catalog consisted of 26 waveforms and it was decomposed into 23 eigenvectors. Figure 4 displays the minimum match, lowest 10% match , highest 10% match and median match of the catalog according to number of eigenvectors used to reconstruct the waveforms. We found the match by first calculating the coefficiants of each eigenvector. We found the values by taking the inner product of the original waveform with each eigenvector. We proceeded to multiply the outputted coefficients times their corresponding eigenvectors to reconstruct the waveform. We then took the noise weighted inner product of the reconstructed waveform and the original to get the match. Figure 5 displays the strength of the normalized eigenvalues to each other and Figure 6 displays the sum of

the squares of the eigenvalues according to how many eigenvectors are used. For the Dimmelmeier 2002 catalog we conclude that the optimal number of eigenvectors to use is five. As shown in Figure 4, the median match at five eigenvectors is .93 and lowest match is .72. The first five eigenvectors also have the strongest eigenvectors is comparison to each other as shown in Figure 5 and describe nearly the entire eigenvalue set as shown in Figure 6. Three example waveforms, each of a different, type overlayed with their match can be seen in Figures 7, 8 , and 9.
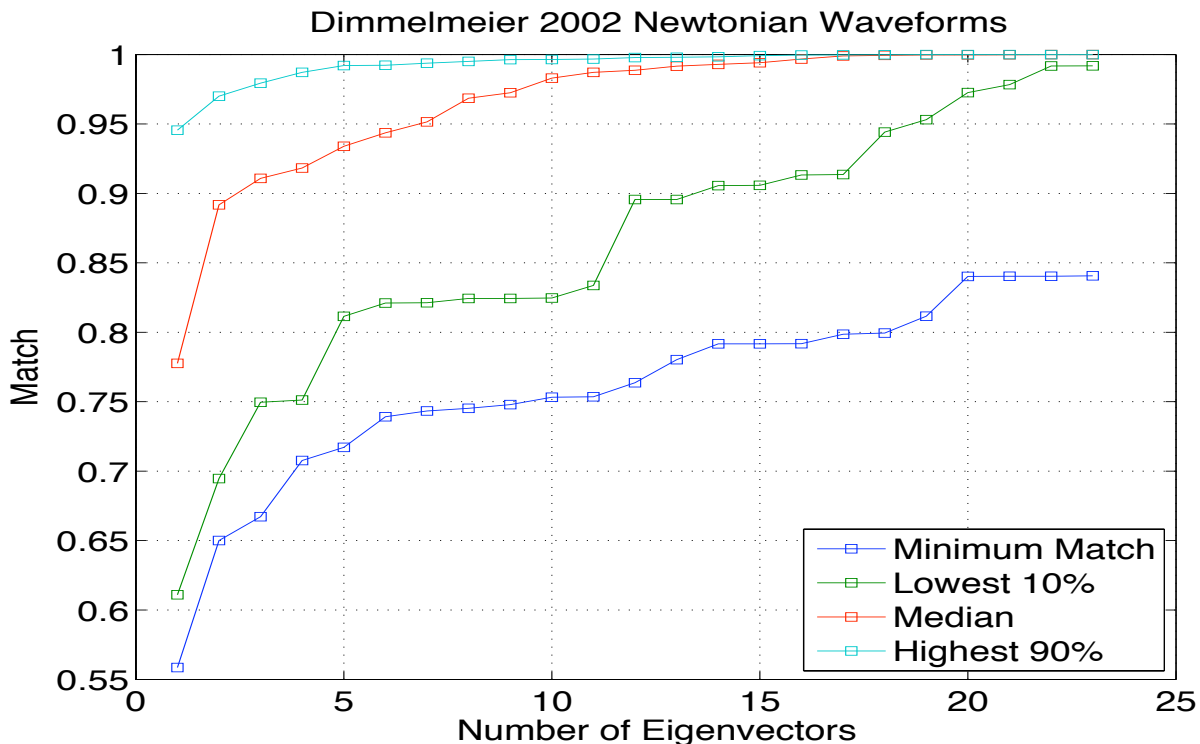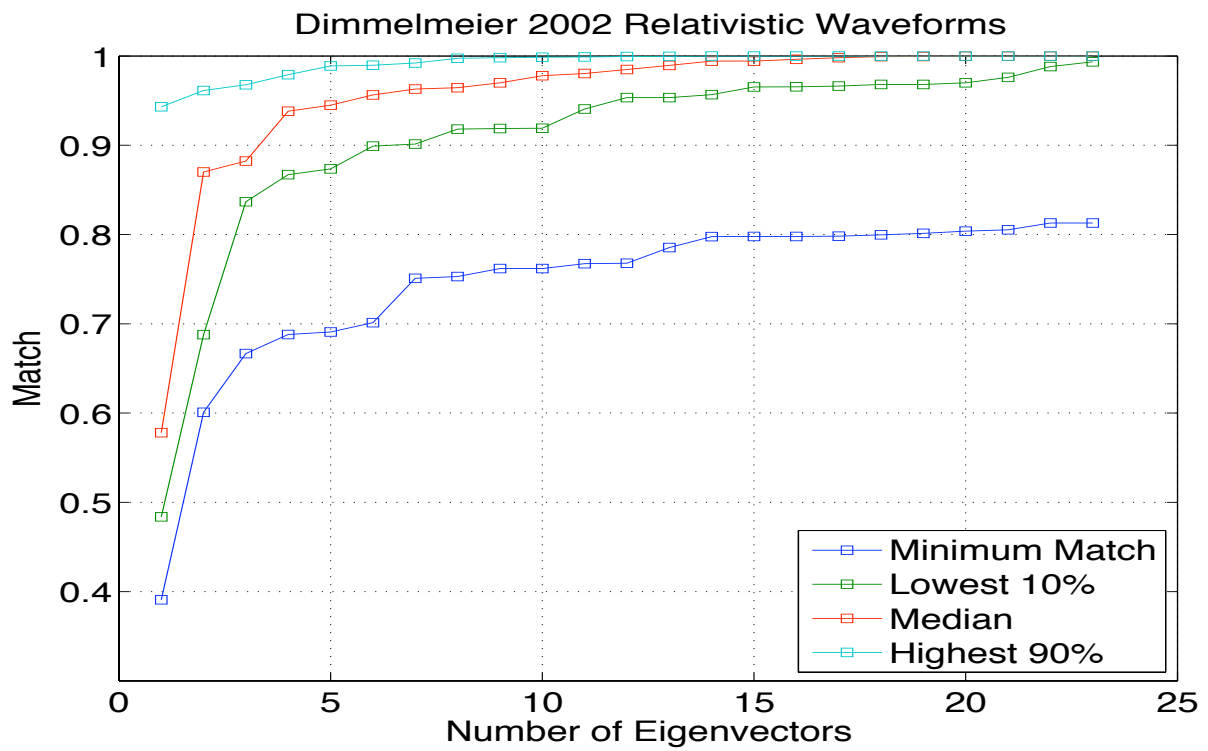

Figure 4: Match of reconstructed waveforms to original according to how many eigenvectors are used. Optimal number of eigenvectors is five

5.2   Dimmelmeier 2002 Relativistic Waveforms

We then produced the same plots for Dimmelmeier's relativistic waveforms in the same catalog. This catalog produced 23 eigenvectors for 26 waveforms. The plots are shown in Figures 10, 11, and 12. We saw that the matches of the waveforms converged much more rapidly than the Newtonian waveforms. This fact concludes that the majority of the relativistic waveforms can be described by less eigenvectors than the Newtonian. This result comes from the fact that the relativistic waveforms look more like each other than the Newtonian. However the minimum match in both cases is around the same at each increment in eigenvectors used which points to each catalog having a waveform that is very different from the others. Due to this fact we chose five eigenvectors to be the optimal number in the relativistic case as well. This number of vectors gave a minimum match of .7 and median match of .95.
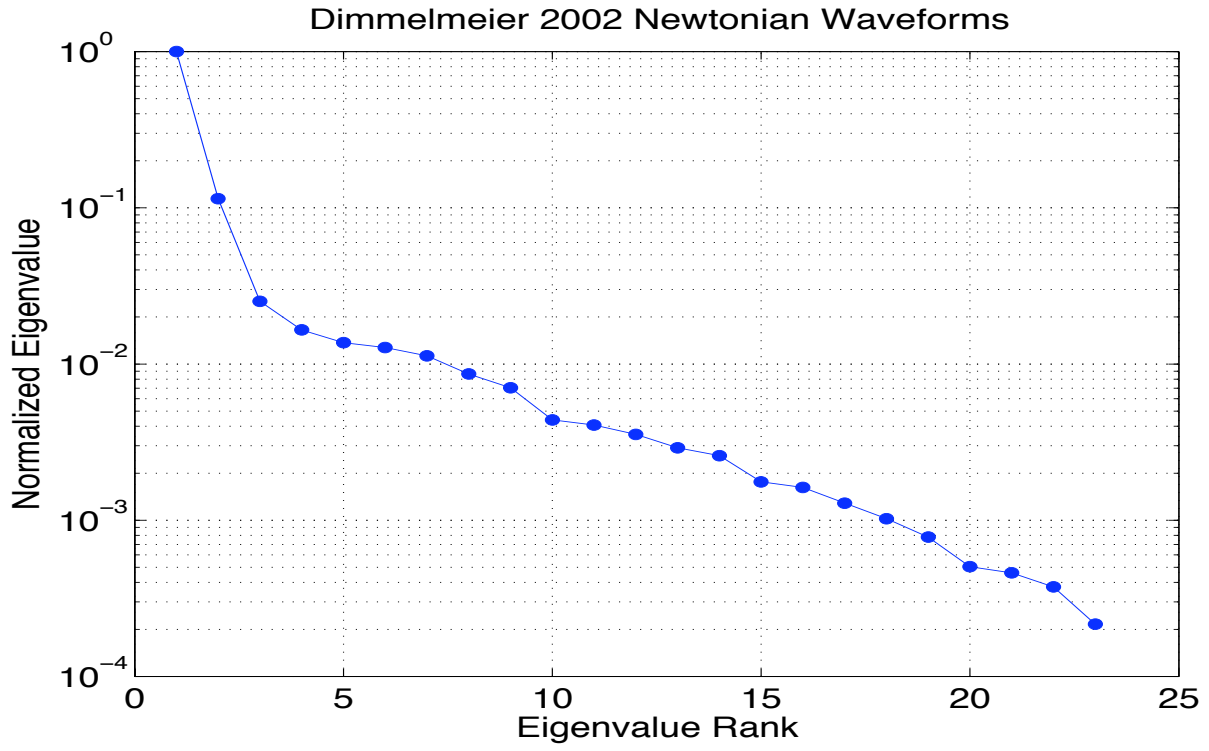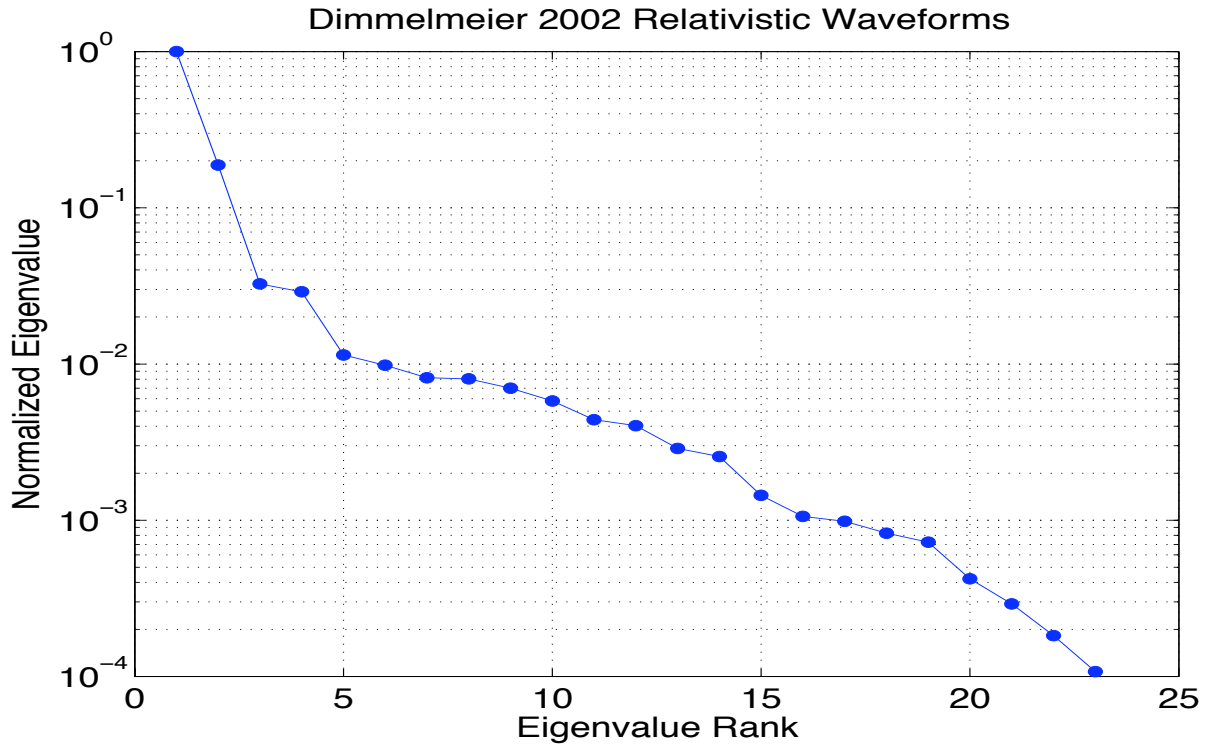
Figure 5: Rank of normalized eigenvectors according to their eigenvalues
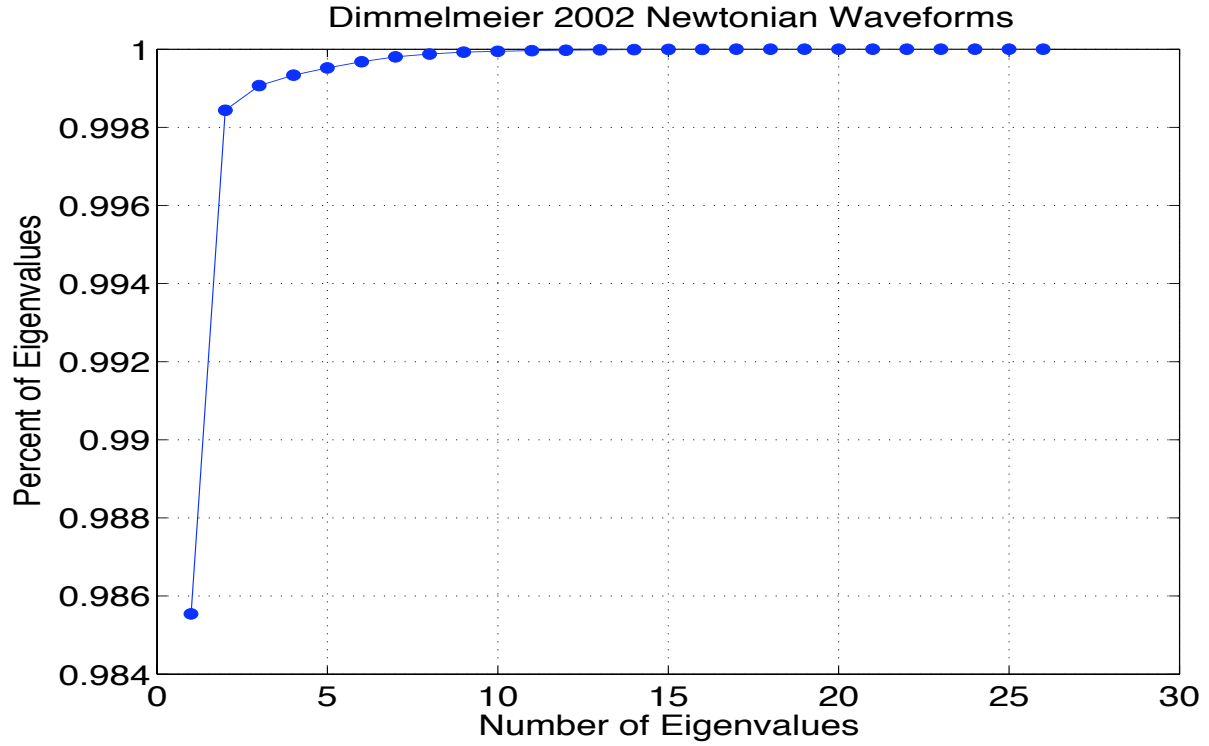
Figure 6: Sum of Squares of Eigenvalues
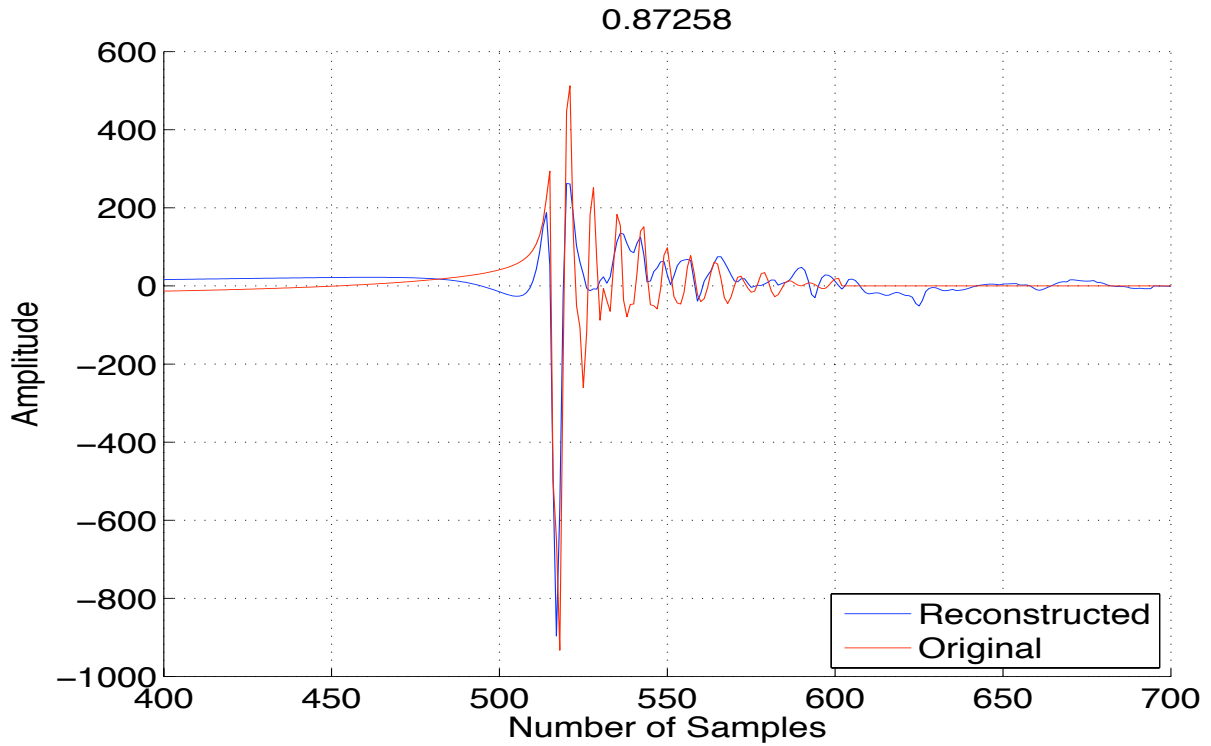
Figure 7: Reconstructed waveform of a Type I with 5 eigenvectors. Inner product match of 0.87258
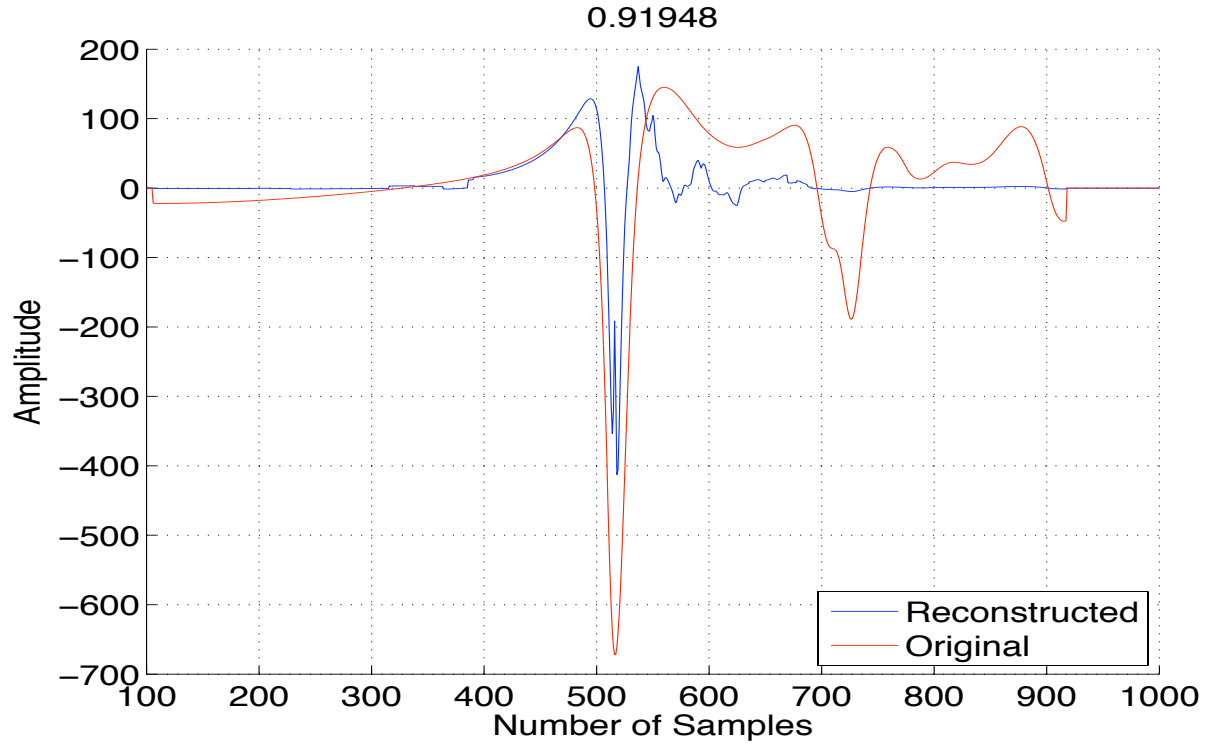
Figure 8: Reconstructed waveform of a Type II with 5 eigenvectors. Inner product match of 0.91948
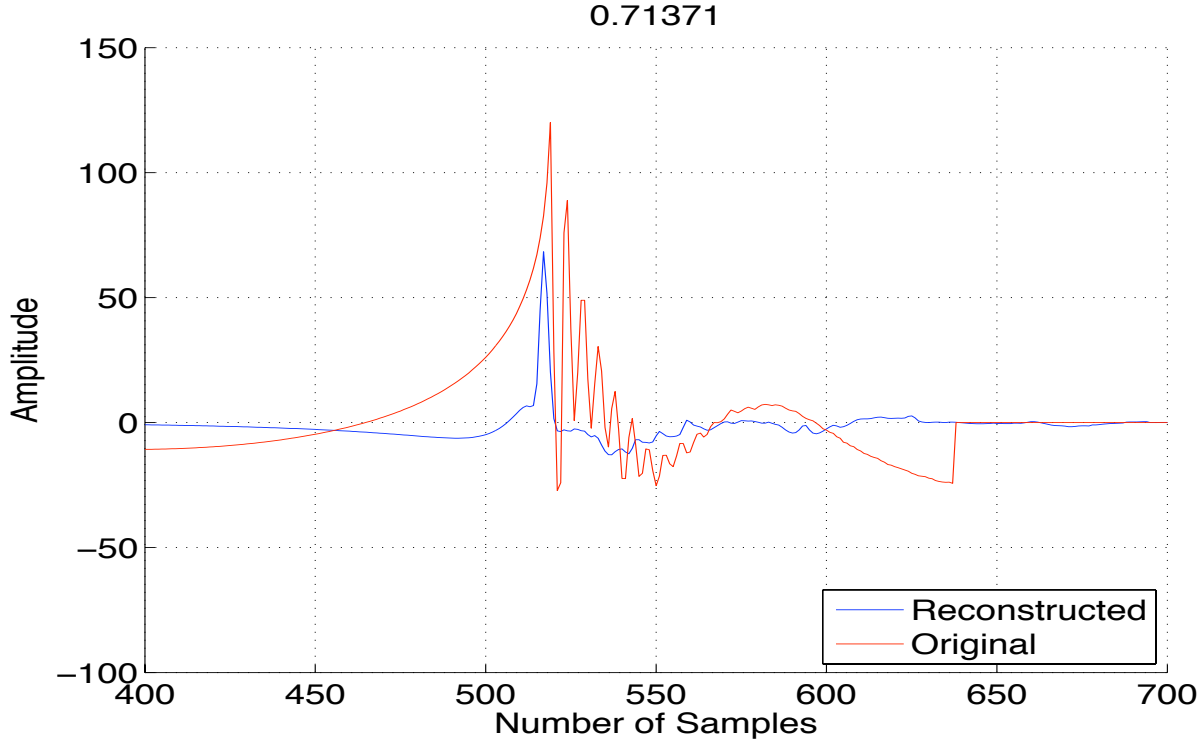
Figure 9: Reconstructed waveform of a Type III with 5 eigenvectors. Inner product match of 0.71371

5.3 Dimmelmeier 2007 Waveforms

Our next catalog was Dimmelmeier's 2007 waveforms. The waveforms in the catalog are simulations of a stellar core collapse to a proto-nuetron star and were generated using a microphysical equation of state and an approximation of deleptonization. All of the waveforms fall in the Type I category. This catalog included 54 waveforms and produced 44 eigenvectors. The plots are seen in Figures 13, 14, and 15. The larger number of waveforms in the catalog made the normalized eigenvalues not as strong as the previous catalogs. This can be seen in Figure 14, where the first eigenvalue is only 5 times stronger than the second where as in previous catalogs the first value was around 10 times stronger. This result is due to the higher sampling of waveforms which makes it more difficult to describe all the waveforms in the samllest number of eigenvectors. In a big catalog we get much more eigenvectors but they are not as strong. Due to this fact, we conclude an optimal number of eigenvectors to be ten, where the median match is .97 and the minimum is .83 (Figure 13).

5.4 Dimmelmeier 2008 Shen Waveforms

Dimmelmeier's 2008 Shen catalog is based on the relativistic field model. It uses an equation of state developed by Shen et al. The catalog contains more Type I waveforms with progenitor masses ranging from 11 to 40 times the mass of the sun. It contains 68 waveforms and produced 51 eigenvectors. The three plots can be seen in Figures 16, 17, and 18. These waveforms gave us nearly the same result as Dimmelmeier's 2007 catalog. We concluded that ten eigenvectors was the optimal number due to the nigh volume of waveforms. However the eigenvalues of this catalog were slightly better then the 2007.

Figure 10: Match of reconstructed waveforms to original according to how many eigenvectors are used. Optimal number of eigenvectors is five

Figure 11: Rank of normalized eigenvectors according to their eigenvalues
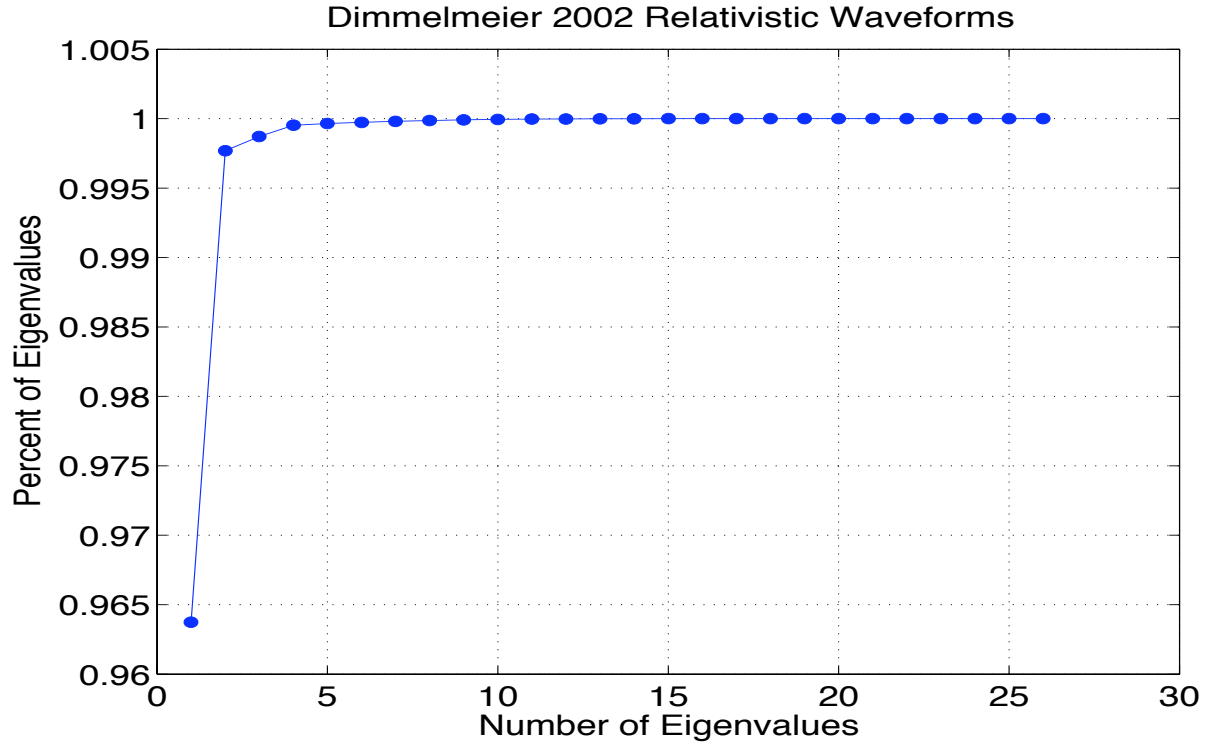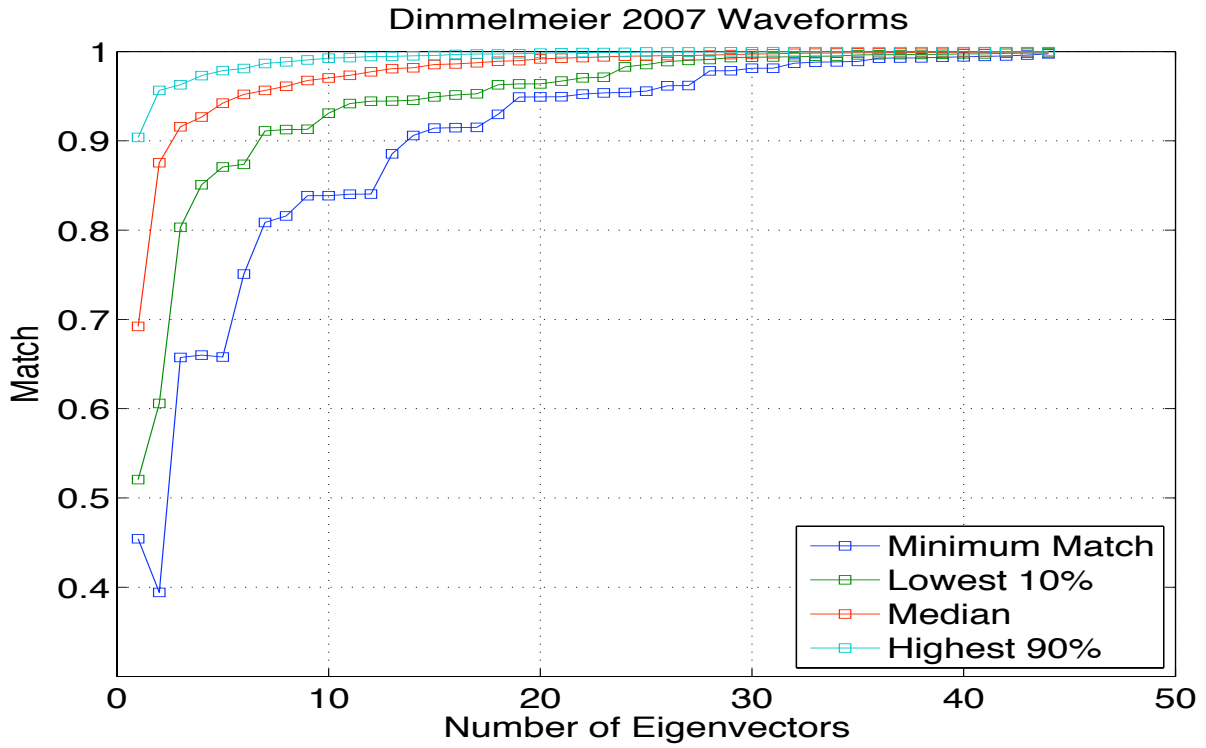

Figure 12: Sum of Squares of Eigenvalues

12

Figure 13: Match of reconstructed waveforms to original according to how many eigenvectors are used
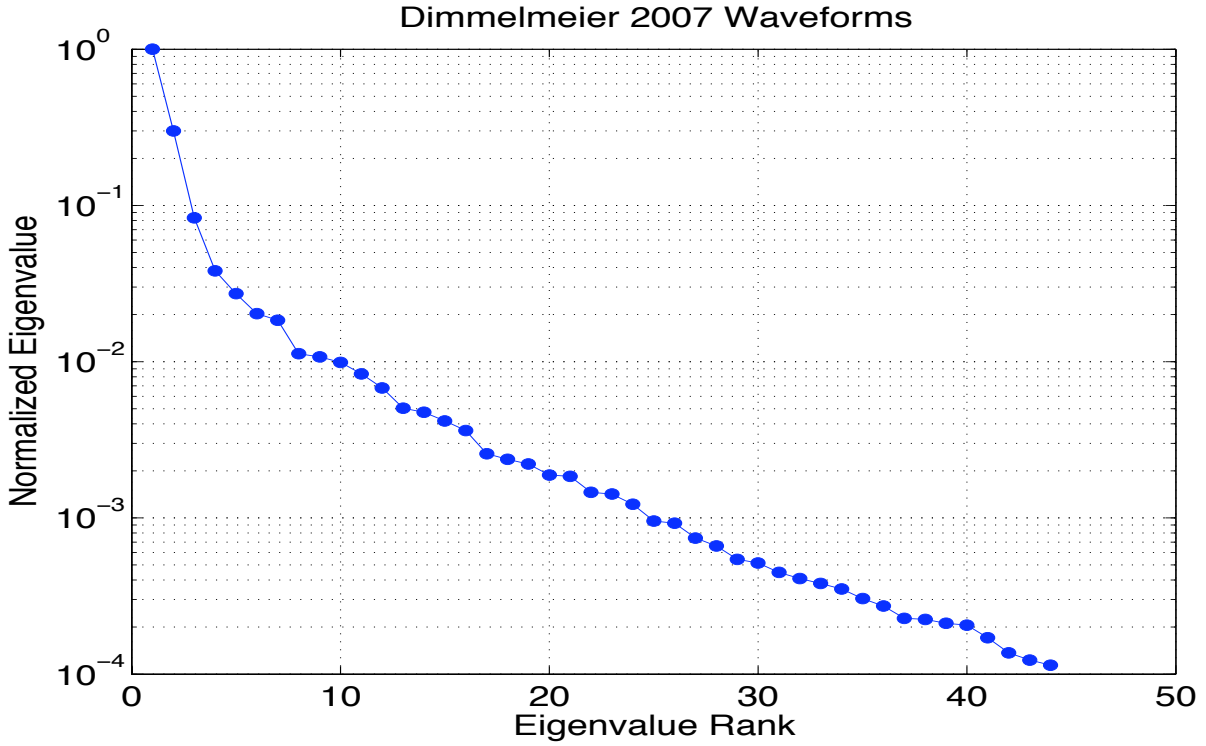

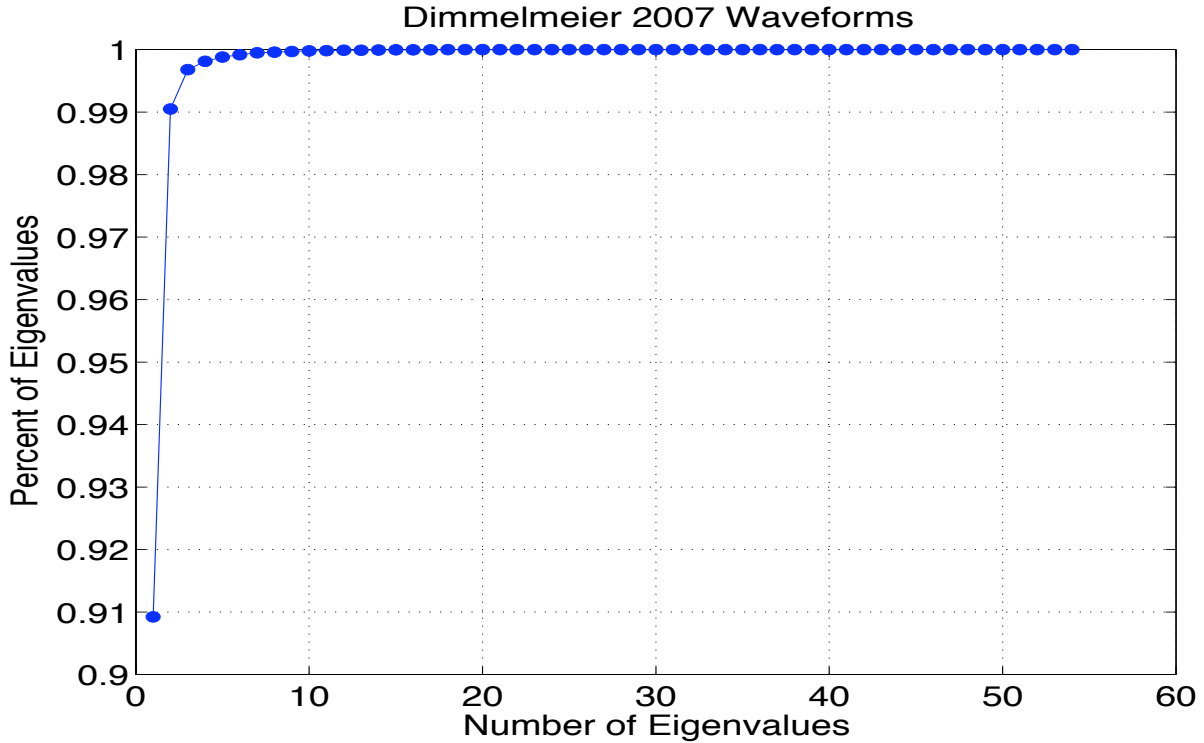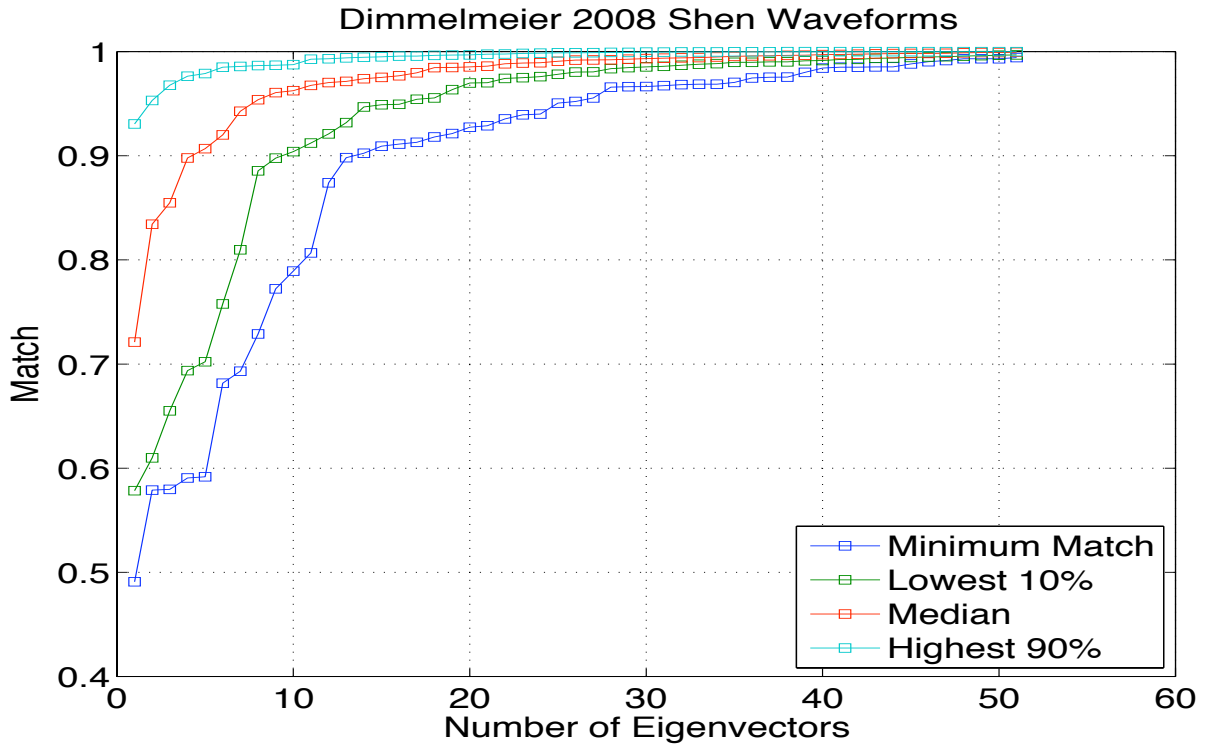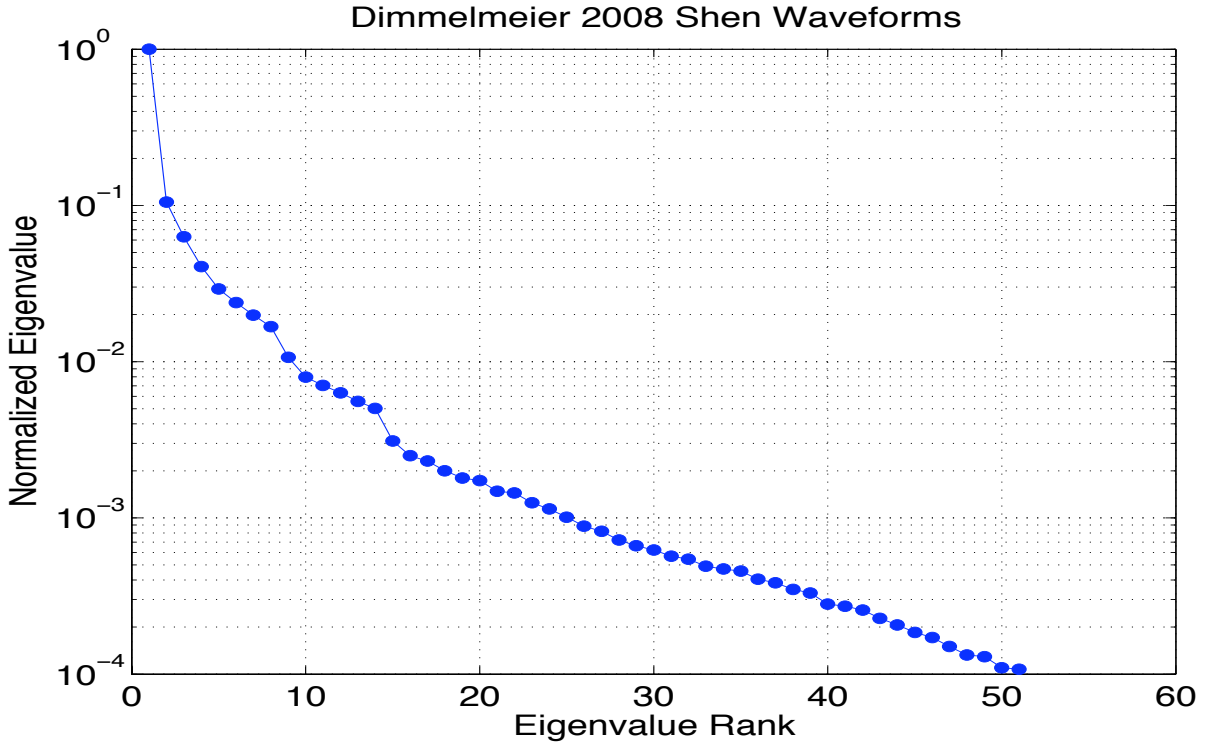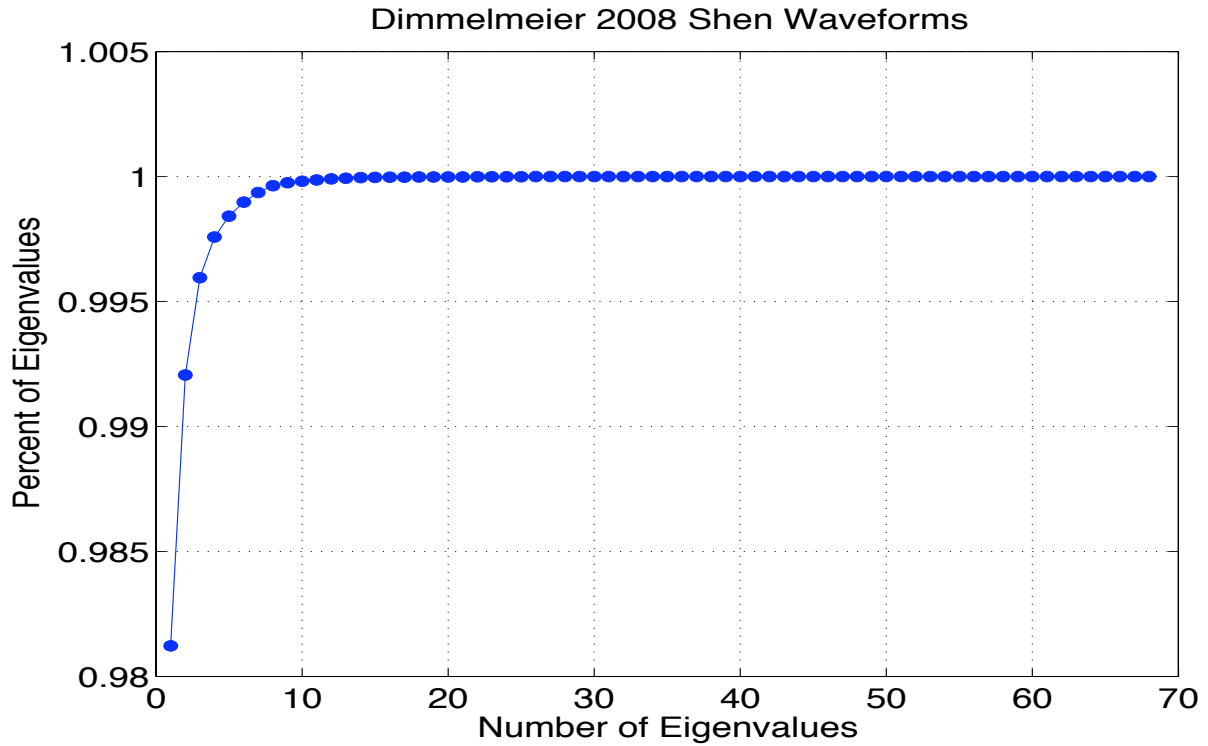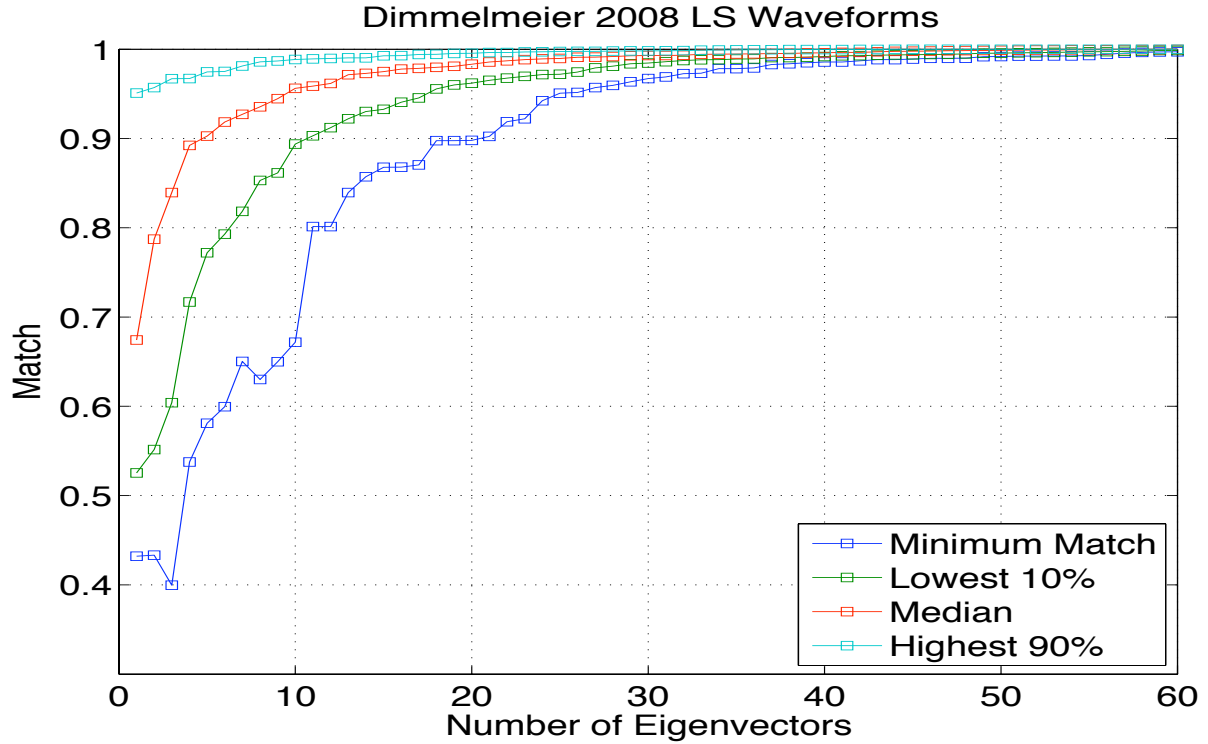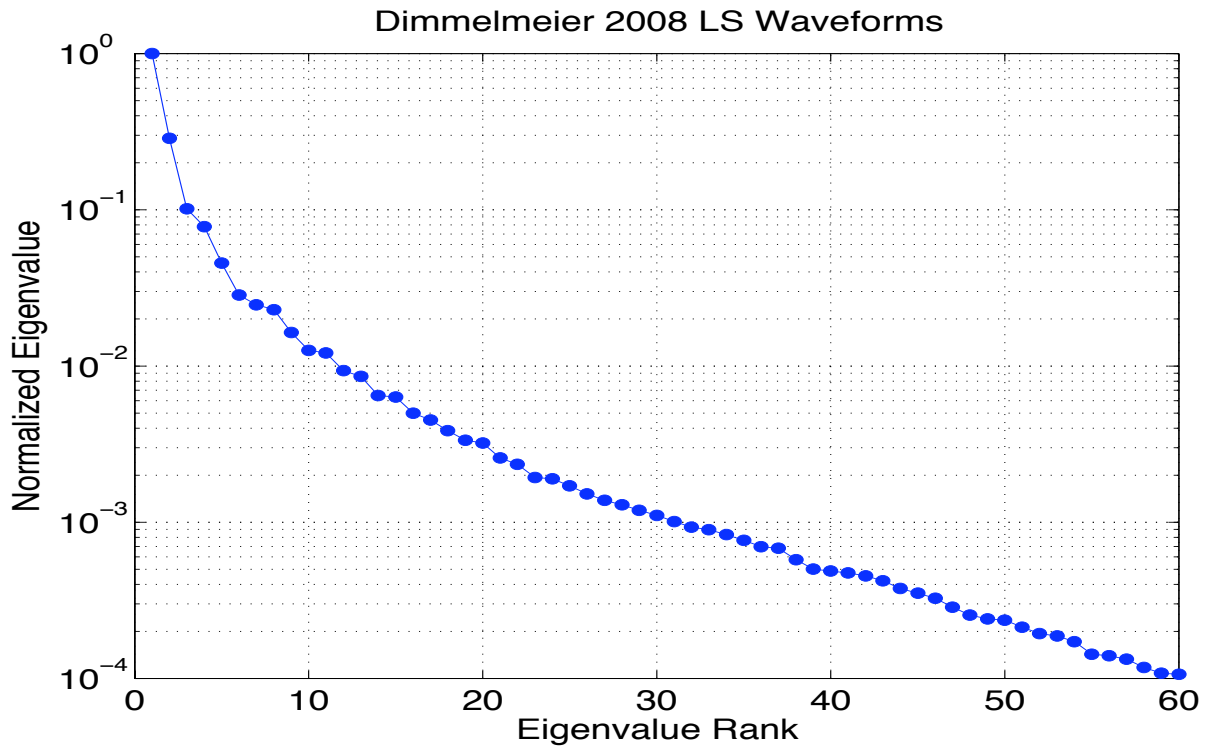Figure 14: Rank of normalized eigenvectors according to their eigenvalues

13

Figure 15: Sum of Squares of Eigenvalues

Ten eigenvectors gave a minimum match of .8 and and median match of .96 (Figure 16).

5.5 Dimmelmeier 2008 LS Waveforms

Dimmelmeier's 2008 LS catalog is based on the compressible liquid drop model. It uses an equation of state developed by Lattimer-Swesty. The catalog also contains more Type I waveforms ranging in progenitor mass. The catalog contains 68 waveforms and produced 60 eigenvectors. The plots can be seen in Figures 19, 20, and 21. The results of this catalog are nearly the same as the Shen waveforms. We chose eleven eigenvectors as the optimal number which gave us a minimum match of .8 and a median match of .96 (Figure 19). The eigenvectors had the same strength as the Shen waveforms.

5.6 Zwerger and Mueller Waveforms

Zwerger and Mueller's catalog contains Type I and Type II waveforms and covers a wide range of initial rotation in the progenitor star. It has 78 waveforms but only produced 37 eigenvectors. This result is due to the fact that many of the eigenvalues were less than one thousandth times as big as the first eigenvalue. The eigenvectors, however, are very strong as can be seen in Figure 23. The plots can be seen in Figures 22, 23, and 24.

Figure 16: Match of reconstructed waveforms to original according to how many eigenvectors are used

Figure 17: Rank of normalized eigenvectors according to their eigenvalues

15

Figure 18: Sum of Squares of Eigenvalues

Figure 19: Match of reconstructed waveforms to original according to how many eigenvectors are used
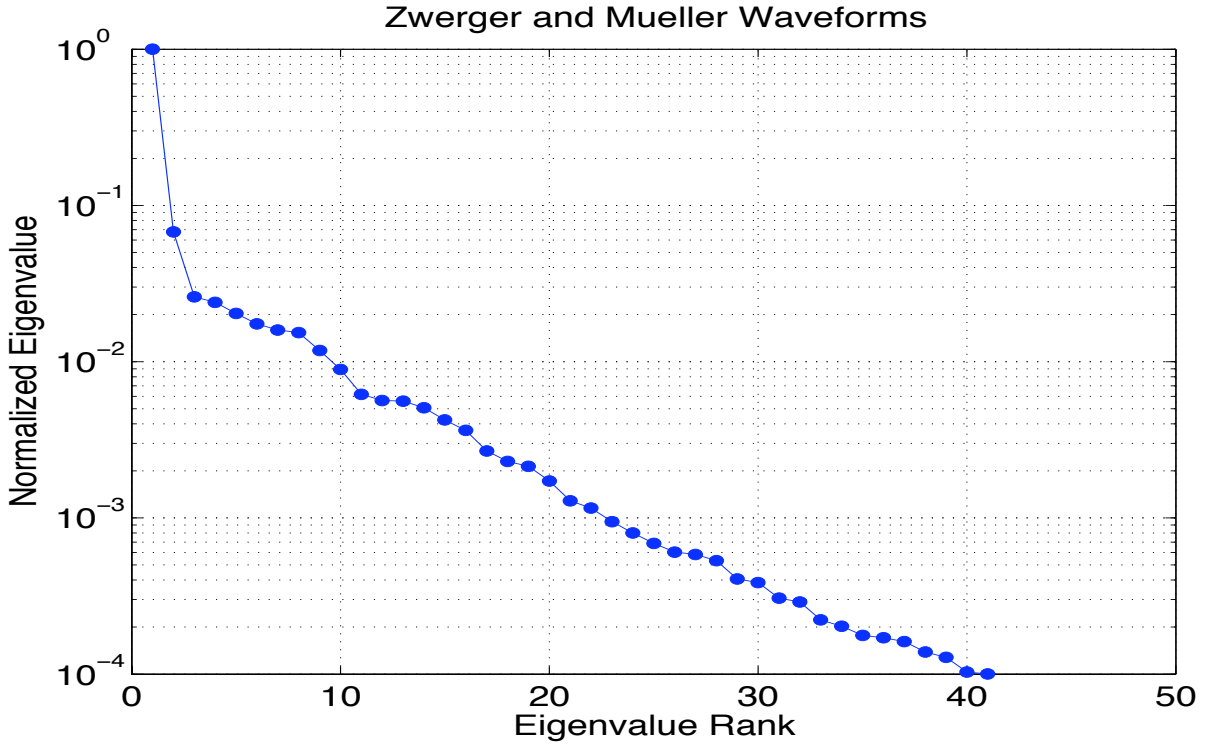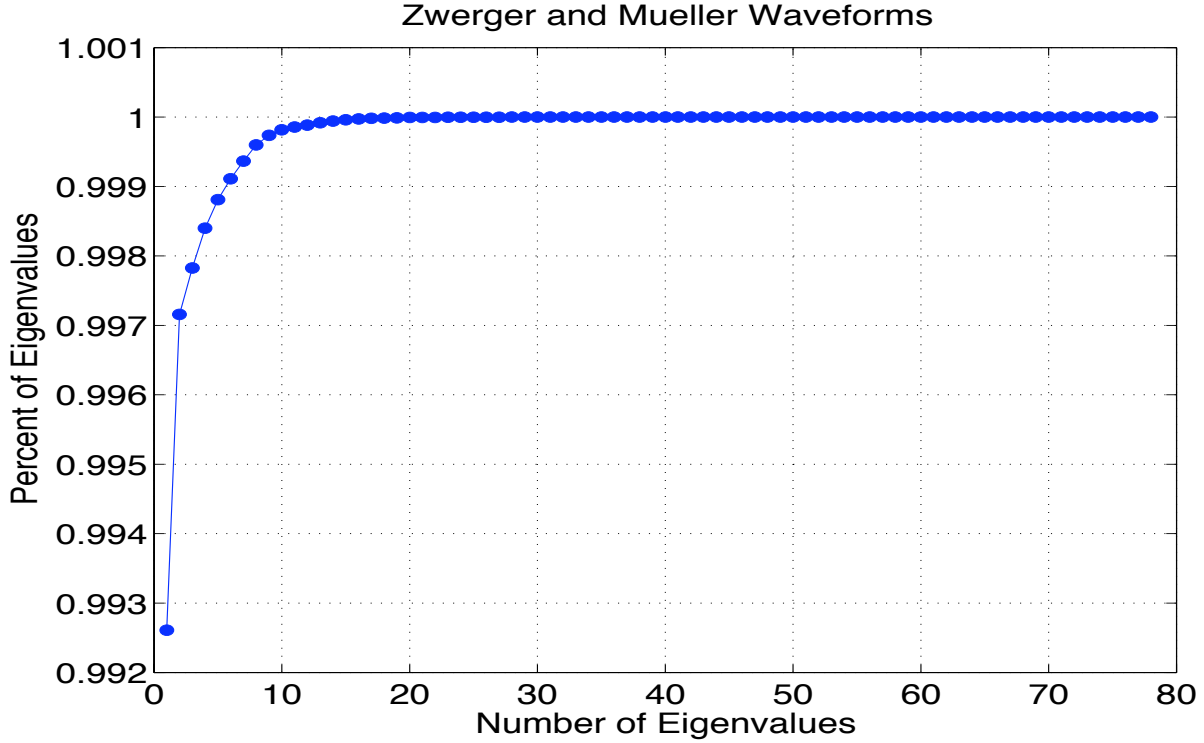
Figure 20: Rank of normalized eigenvectors according to their eigenvalues
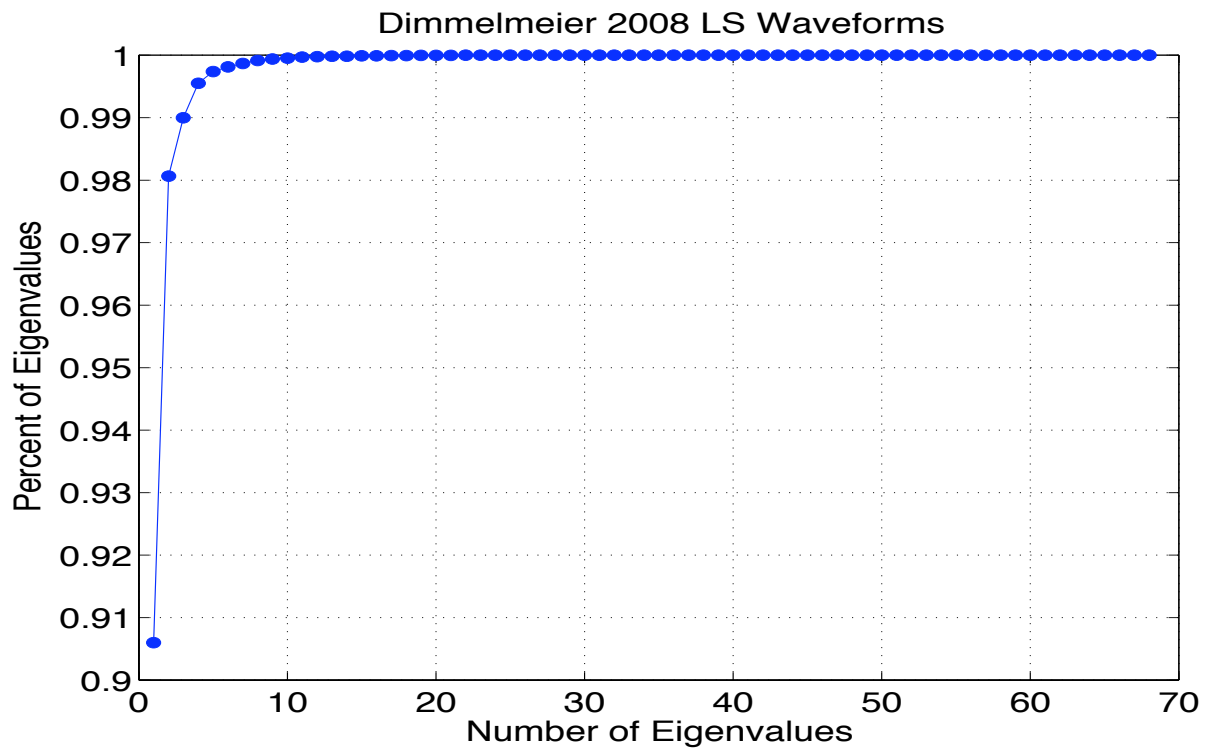
Figure 21: Sum of Squares of Eigenvalues

17
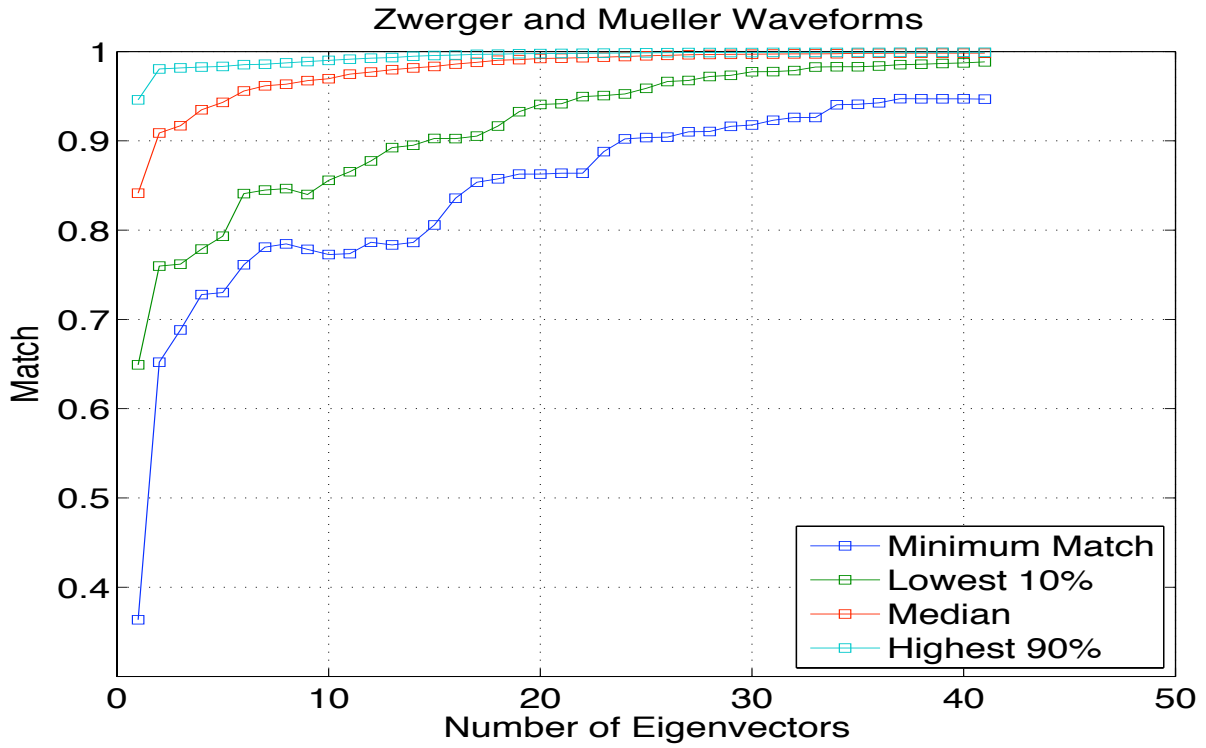
Figure 22: Match of reconstructed waveforms to original according to how many eigenvectors are used

Figure 23: Rank of normalized eigenvectors according to their eigenvalues

18

Figure 24: Sum of Squares of Eigenvalues

5.7 Ott and Burrow Waveforms

Ott's and Burrow's waveform catalog are produced from a two dimensional axis symmetric purely hydrodynamical simulations of rotating stellar core collapse. These waveforms also rely on Lattimer-Swesty equations of state. It also does not take into account microphysics such as electron capture. Ott and Burrow's catalog had very interesting results in the matches of reconstructed waveforms to original. The plots are seen in Figures 25, 26, and 27. As seen in Figure 25, the minimum match doesn't converge until the last few eigenvectors are added. This result is due to the fact that there are two waveforms in the OBcat catalog that have very different features compared to the other waveforms. Due to this fact we chose ten eigenvectors as the optimal number since the two odd waveforms looked very different from the rest.

5.8 All Waveforms

We combined all of the waveform catalogs into one big catalog of 374 waveforms. This input resulted in 39 output eigenvectors. As shown in Figure 28, the minimum match never converges past .5. This result is due to the few waveforms in the catalogs which contain features unlike the rest. However the median match reaches .83 by five eigenvectors which we decided was optimal. At five eigenvectors, the lowest 10% match is at .65 which shows that 90% of the 300 waveforms can be described with nearly 70% accuracy using only five eigenvectors. Figure 29 shows that the first few eigenvectors are also very strong. The first eigenvector is about ten times stronger than the second and the second is around 5 times stronger than the third. The sum of the squares plot also shows the eigenvalues converging very rapidly to one (Figure 30).
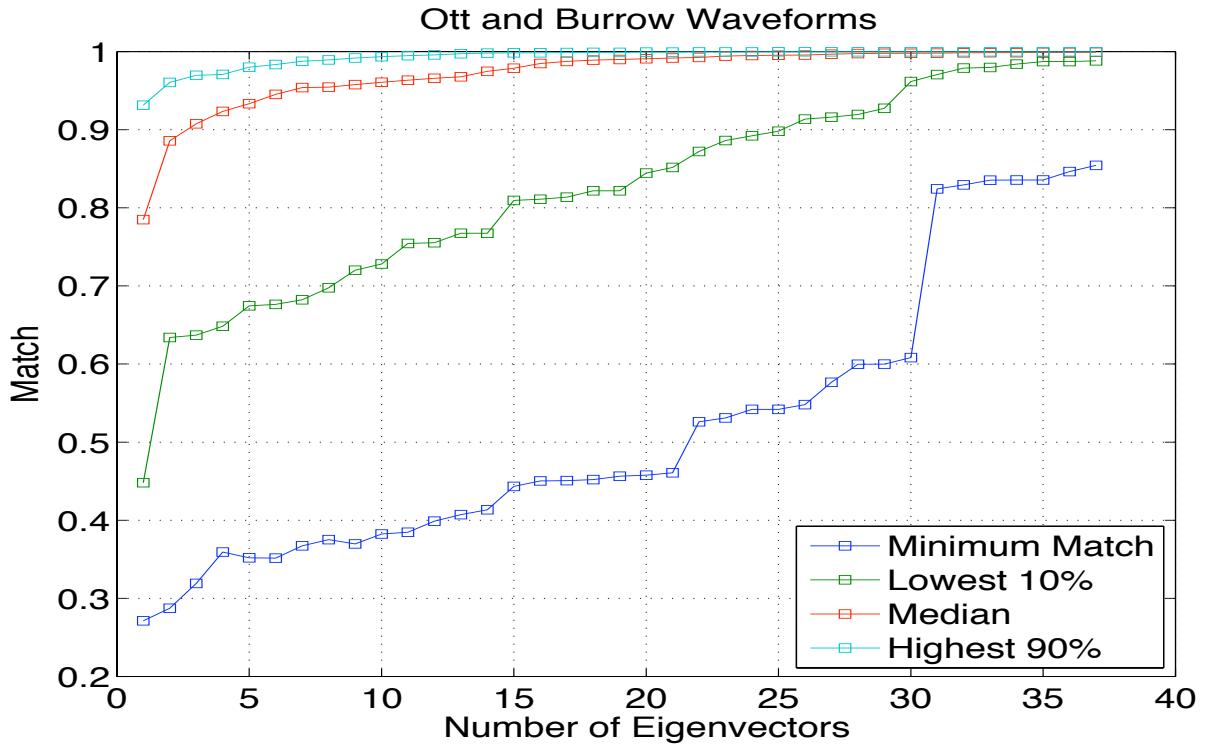
Figure 25: Match of reconstructed waveforms to original according to how many eigenvectors are used
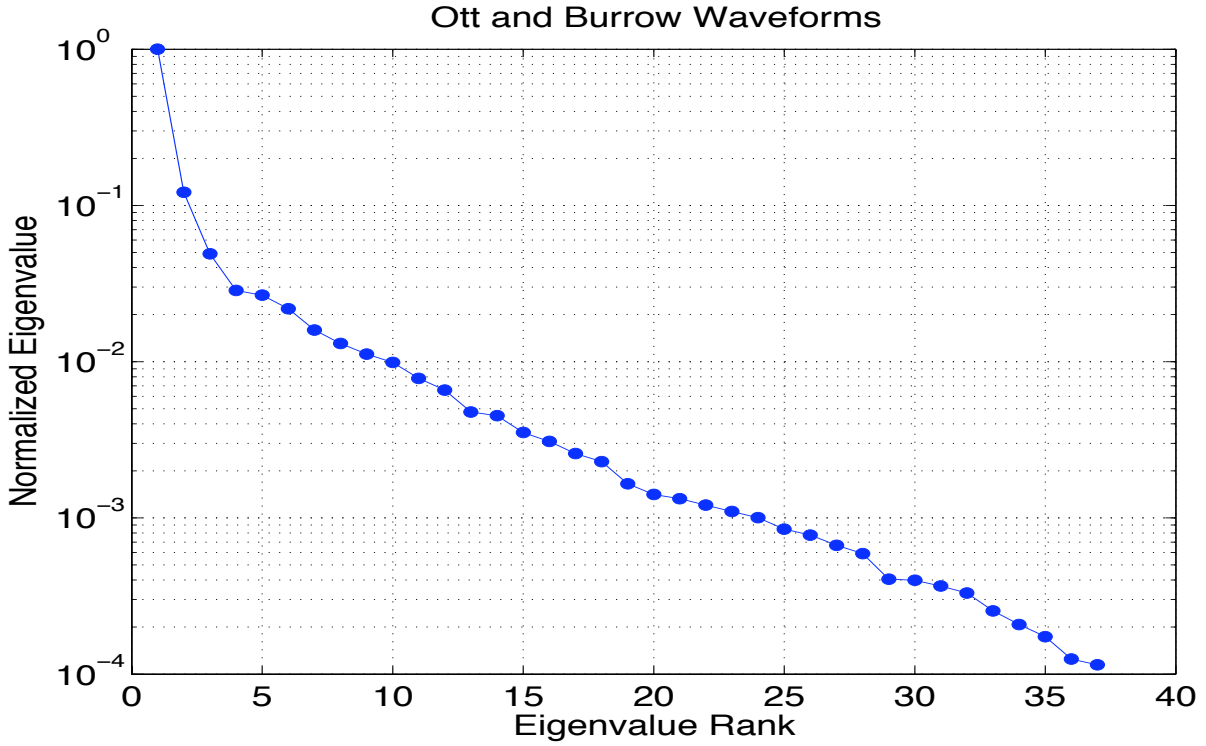

Figure 26: Rank of normalized eigenvectors according to their eigenvalues
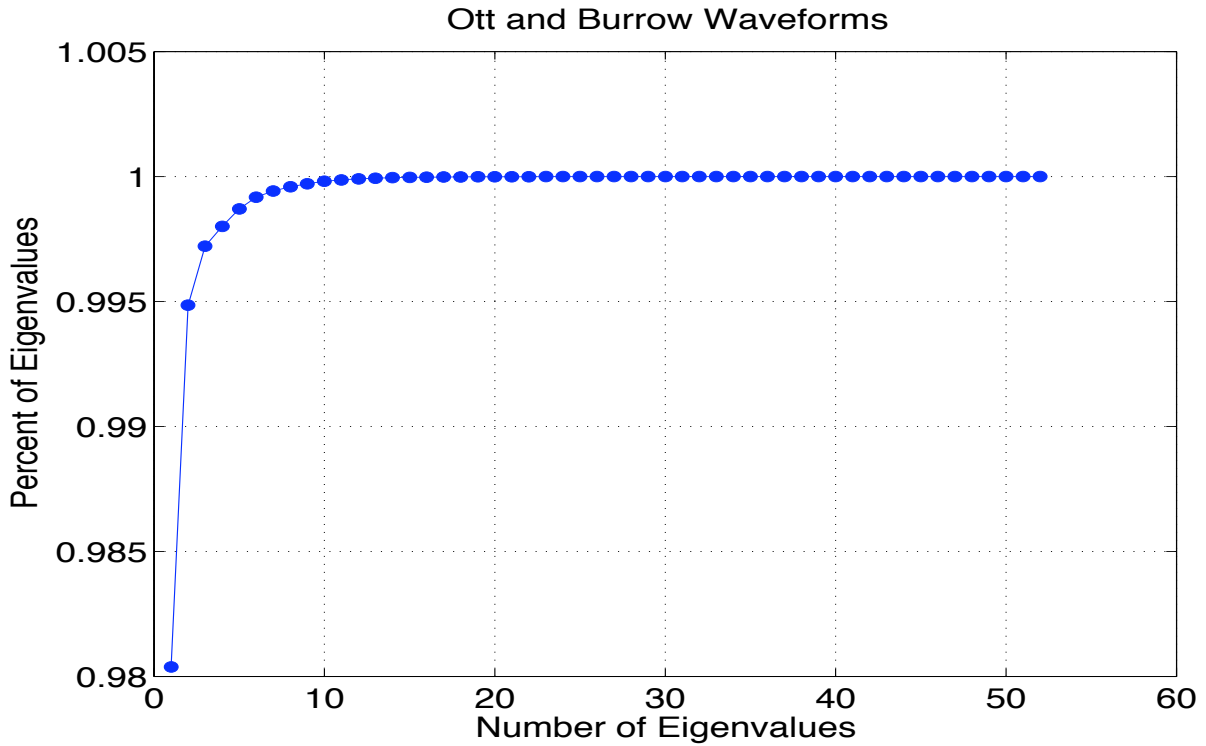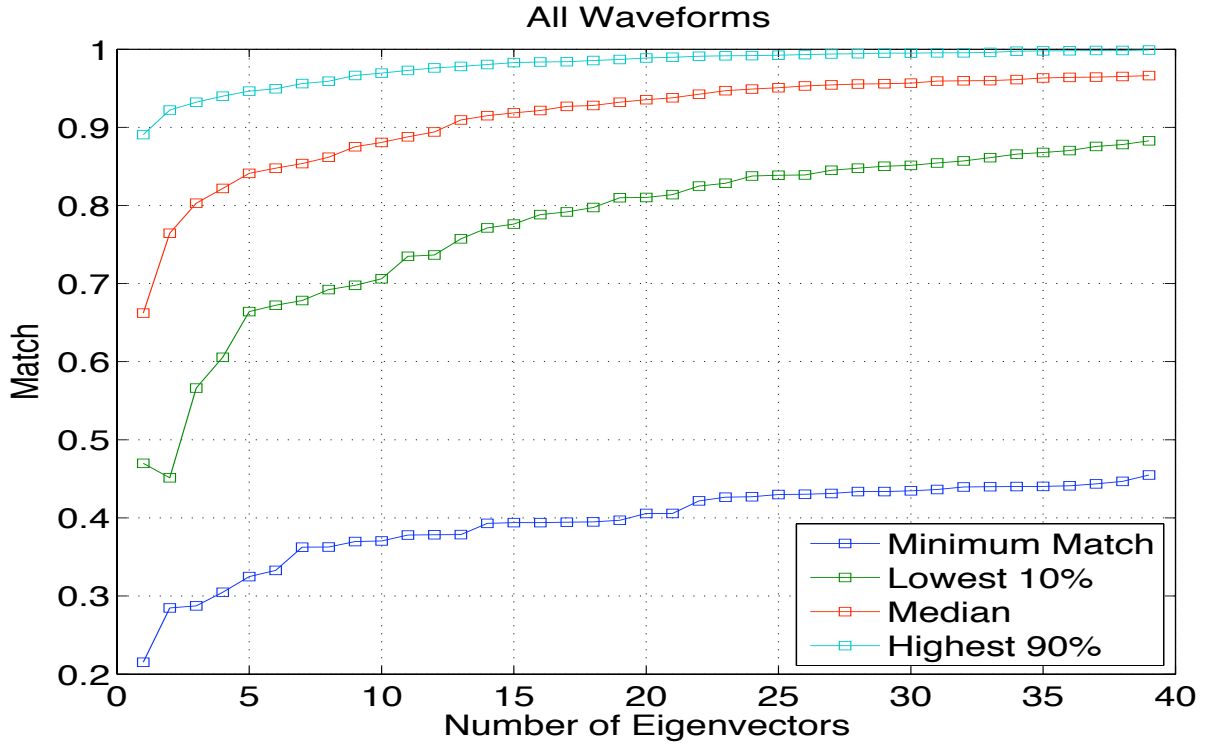
Figure 27: Sum of Squares of Eigenvalues

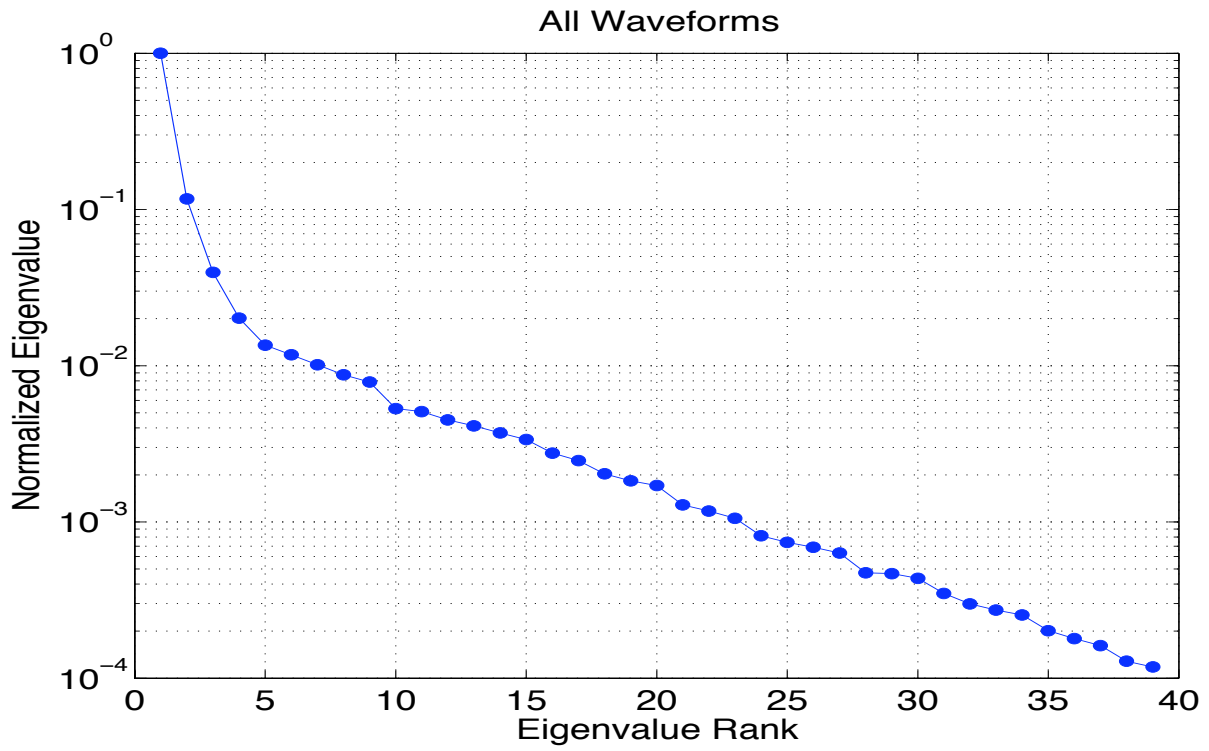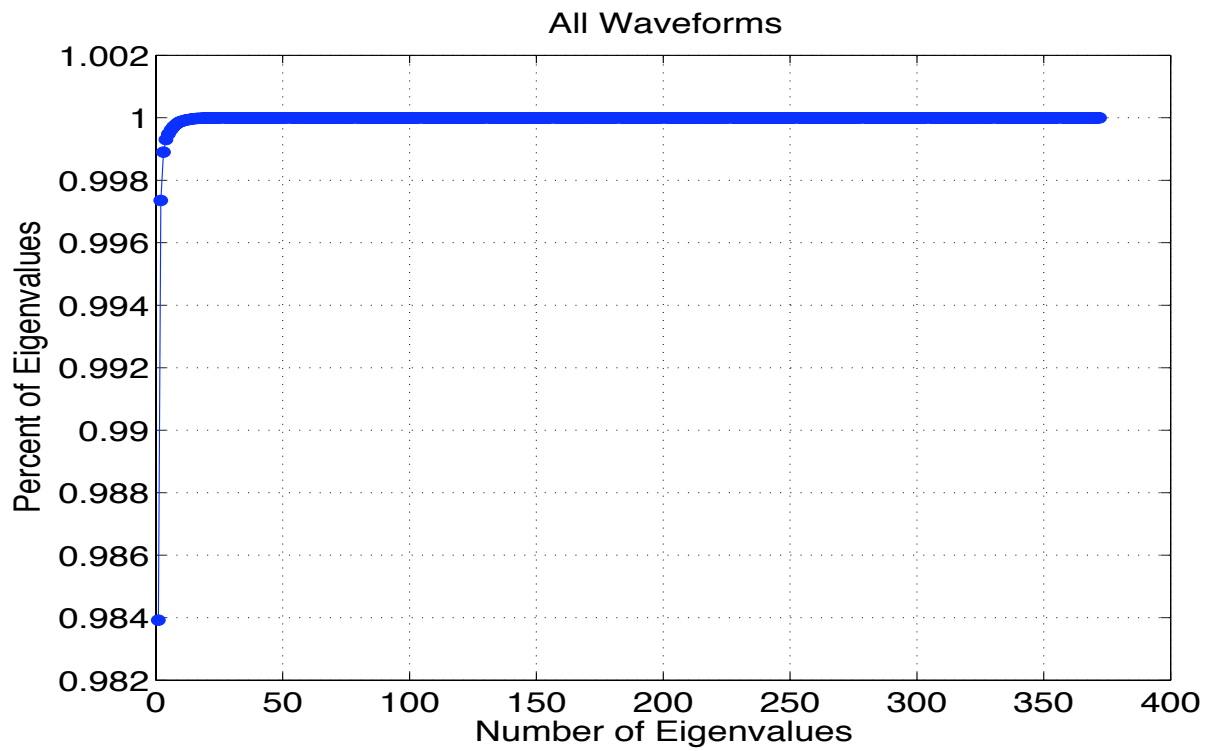Figure 28: Match of reconstructed waveforms to original according to how many eigenvectors are used

Figure 29: Rank of normalized eigenvectors according to their eigenvalues

Figure 30: Sum of Squares of Eigenvalues

22

6 Classification of Waveforms

The next step in our project was to determine if we could classify waveforms using the coefficients of the eigenvectors used to reconstruct the waveforms. We first calculated the coefficients of the eigenvectors by taking the inner product of the original waveform with each eigenvector. We then found the correlation between each waveform's coefficients to find any patterns. We chose to use Dimmelmeier's 2002 catalog because it contains all three types of waveforms. We found the coefficients of the eigenvectors do correlate with the type of waveform. Below in Figures 31 and 32 are two Type I waveforms from the catalog. We found the correlation of their coefficients after using 10 eigenvectors to be .9917 (Figure 33). We also found a strong correlation between Type II and Type III waveforms which can be seen in Figures 34, 35, 36 and Figures 37, 38, 39. We found a correlation of .9617 between two Type II waveforms and a correlation of .8512 between two Type III waveforms.
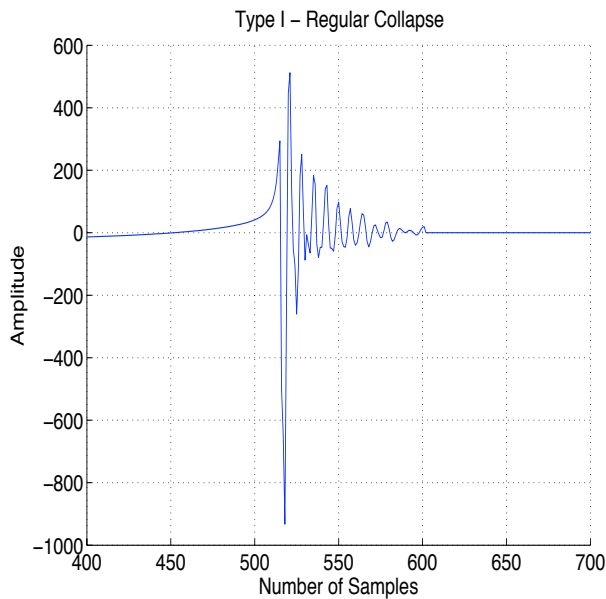

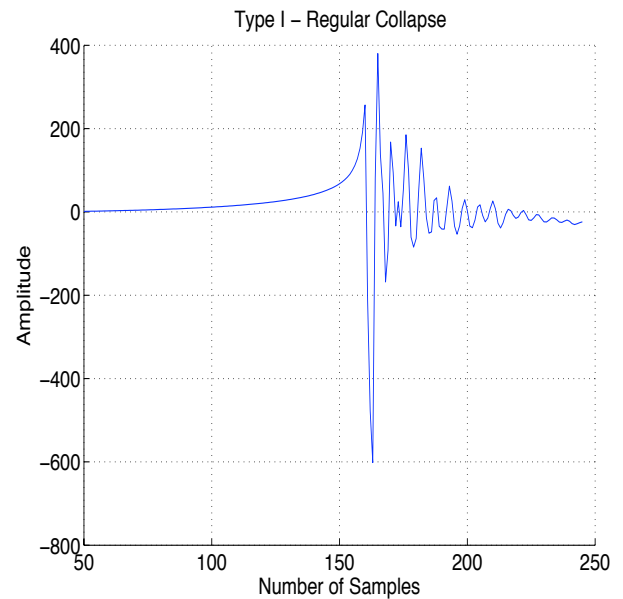Figure 31: Type I waveform from Dimmelmeier 2002 Catalog

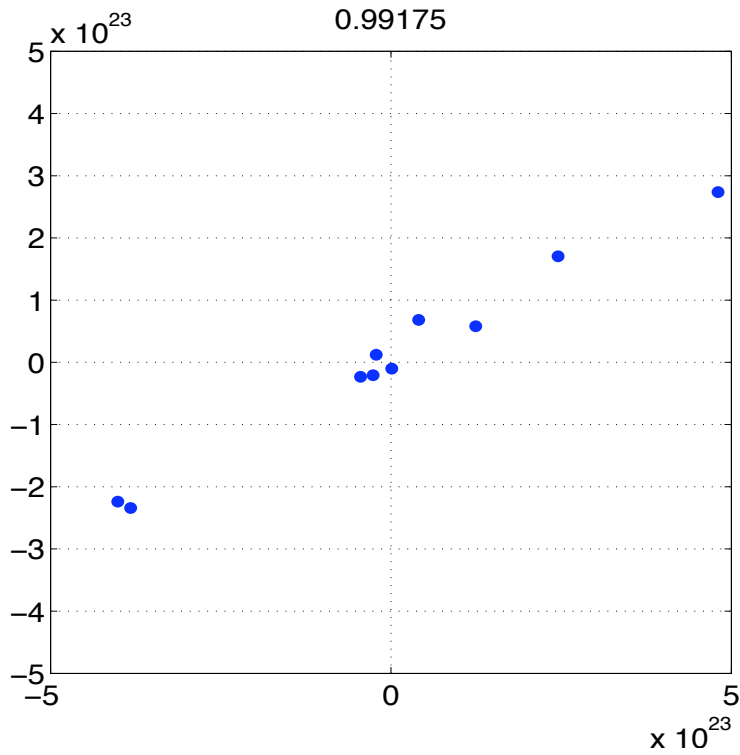Figure 32: Type I waveform from Dimmelmeier 2002 Catalog

0.99175

Figure 33: Correlation of the coefficients corresponding to the 10 eigenvectors used
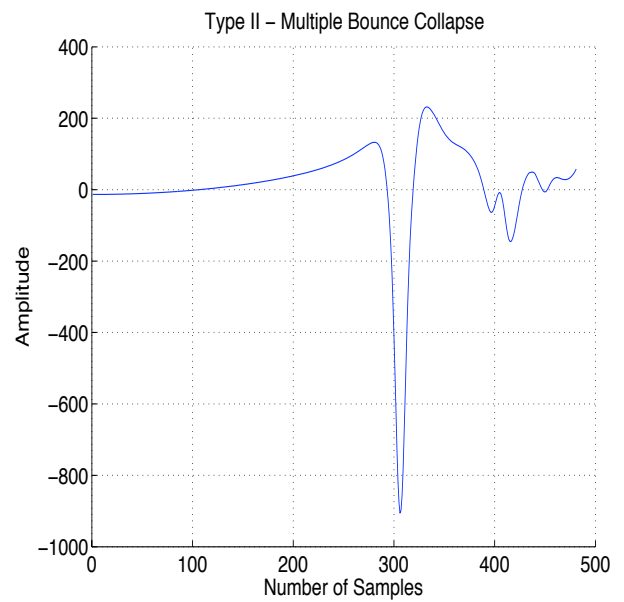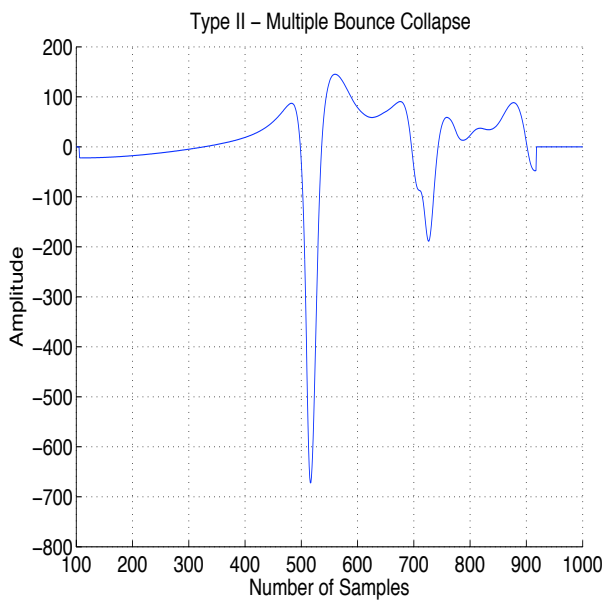

Figure 34: Type II waveform from Dimmelmeier 2002 Catalog

Figure 35: Type II waveform from Dimmelmeier 2002 Catalog

7   Conclusion

The results shown above provide very practical applications to the field of gravitational waves. Most of the catalogs tested can be decomposed into five eigenvectors which allows for quick classification of a detected waveform. The coefficients of the
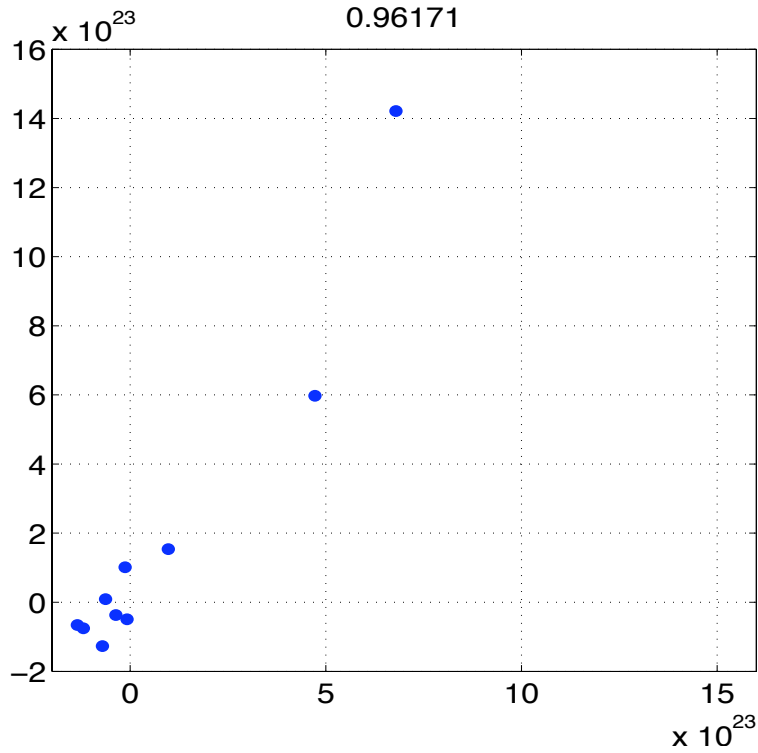
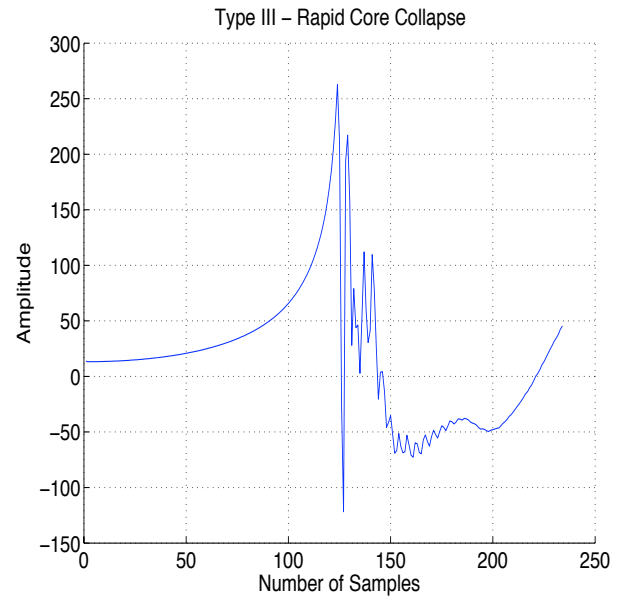Figure 36: Correlation of the coefficients corresponding to the 10 eigenvectors used
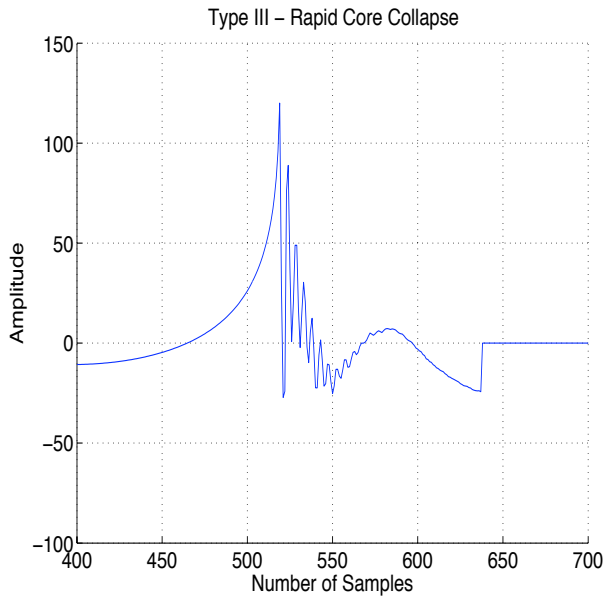

Figure 37: Type III waveform from Dimmelmeier 2002 Catalog

Figure 38: Type III waveform from Dimmelmeier 2002 Catalog

eigenvectors used to reconstruct the waveforms can very accurately determine the type of the waveform. More catalogs are currently being used in our decomposition to see if further parameters, such as initial mass and rotation, can be deduced from the coefficients. The waveforms used in this paper were entirely of the core-bounce type so adding a wider variety of
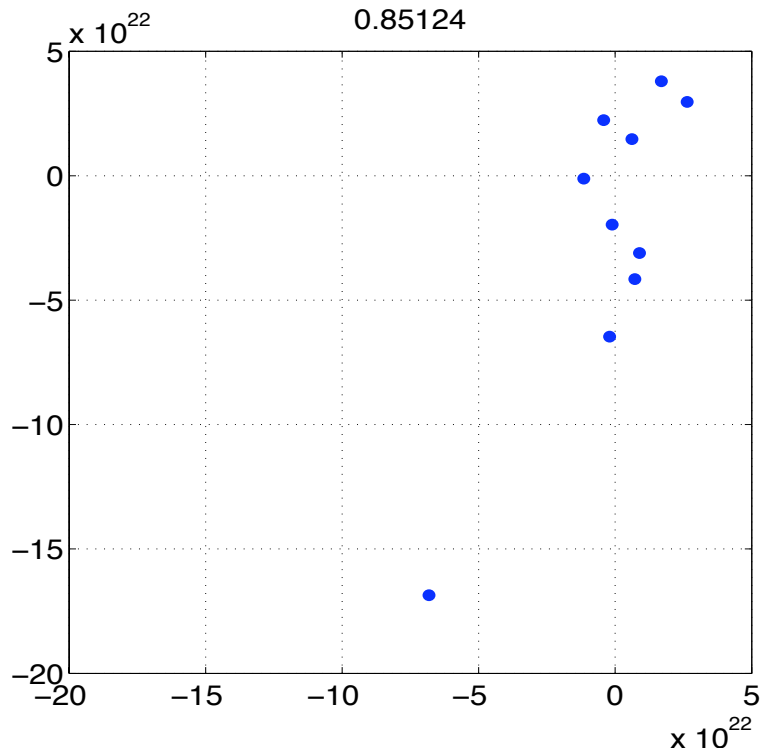
Figure 39: Correlation of the coefficients corresponding to the 10 eigenvectors used

collapse mechanisms will give us better results.

References

Dimmelmeier, H., Font, J. A., & Müller, E. 2002, , 388, 917

Dimmelmeier, H., Ott, C. D., Janka, H.-T., Marek, A., & Müller, E. 2007, Physical Review Letters, 98, 251101

Dimmelmeier, H., Ott, C. D., Marek, A., & Janka, H.-T. 2008, , 78, 064056

Heng, I. S. 2009, Classical and Quantum Gravity, 26, 105005

Ott, C. 2003,

Ott, C. D., Burrows, A., Livne, E., & Walder, R. 2004, , 600, 834

Zwerger, T., & Mueller, E. 1997, , 320, 209